Comparing wave transformation of a hard, impermeable structure with various biogenic, permeable structures

Results of an experimental flume study

---

by

Jan Tervoort

Utrecht University

Master Thesis Marine Sciences

Student ID: 2500167

Date: 10-06-2022

Supervisors: Jim van Belzen and Tjeerd Bouma

Acknowledgement

I would first like to thank and acknowledge my supervisor Jim van Belzen for all the guidance, help, and support during this thesis project. Additionally, I would like to thank my other supervisor Tjeerd Bouma for the useful feedback during the presentation.

Besides, a special thanks to the NIOZ-staff for using their facilities and materials. Especially Jaco de Smit and Martijn Hofman for helping me with the experiment set-up.

Finally, I would also like to thank Ward Pennink, a friend who helped me with programming-related issues.

Abstract

Intertidal areas worldwide are threatened by man-made basin alterations, boat-wakes, and sea-level rise, resulting in changed sediment dynamics and a process called sediment starvation. Traditionally, hard and impermeable structures are constructed on intertidal foreshores to attenuate wave energy and restore the disbalance in sediment dynamics. However, wave reflection and scouring in front of the structure are reasons why there is a growing consensus toward more permeable and biogenic structures in coastal defence schemes. The assessment of the interaction of waves with these permeable structures is limited in the literature. This flume study quantified and compared wave attenuation, reflection, and scouring potential of different-sized gabions filled with empty oyster shells, empty mussel shells, loose brushwood, and bundled brushwood to a hard brick stone structure under varying hydrodynamical conditions. The results show that consistent differences in wave attenuation were hardly observed between hard and biogenic materials. The emerged mussel structure even attenuated wave energy best for low submergence ratios. Emerged hard structures with low submergence ratios did generate up to 46.2% more wave reflection than the various biogenic structures for incident short-period waves. There was also a higher bed shear stress under wave action measured just before the emerged hard structure. Additionally, the correlation between wave reflection/attenuation and relative submergence showed a large spread, highlighting the importance of incident wave characteristics in describing this correlation. The findings demonstrate why there is increasing attention to using biogenic structures to protect intertidal areas from sediment starvation and can be used as guidelines for implementation under natural conditions.

Table of contents

List of symbols

Abbreviation	Definition	Unit
B	Crest width	cm
d	Rock diameter	cm
d_s	Depth of submergence	cm
f	Frequency	Hz
f_w	Friction parameter	-
H_0	Incident wave height	cm
H_r	Reflected wave height	cm
H_s	Spectral significant wave height	cm
H_t	Transmitted wave height	cm
h	Water depth	cm
h_s	Structure height	cm
k	Wave number	cm^{-1}
k	Intrinsic permeability	m^2
K_l	Dissipation coefficient	-
K_r	Reflection coefficient	-
K_t	Transmission coefficient	-
L	Wavelength	cm
n	Porosity	-
p	Pressure	Pa
ρ	Density	kg m^{-3}
q	Flow velocity	m s^{-1}
RS	Relative submergence	-
SR	Submergence ratio	-
t	Wave period	s
τ	Bed shear stress	J m^{-3}
TKE	Turbulent kinetic energy	J m^{-3}
V_p	Pore volume	m^3
V_t	Total volume	m^3
u	Flow velocity (x-direction)	m s^{-1}
v	Flow velocity (y-direction)	m s^{-1}
w	Flow velocity (z-direction)	m s^{-1}
μ	Fluid viscosity	Pa s
ω	Angular velocity	rad s^{-1}

1 Introduction

There is a growing consensus on the importance of intertidal areas due to their high ecological and economic value (Borsje et al., 2011; Bouma et al., 2014; King & Lester, 1995; Morris et al., 2018; Temmerman et al., 2013; Walles et al., 2016). Simultaneously, sea-level rise, boat-wakes, and man-made basin alterations put pressure on those areas (Boersema et al., 2015; Herbert et al., 2018). The construction of dams, storm surge barriers, and other artificial interventions often lead to decreased sediment supply from the sea to the tidal inlets (Boersema et al., 2015). A decrease in tidal energy further limits the resuspension and transport of sediment from the gullies to the tidal flats and marshes (Boersema et al., 2015). Reduced fluvial deposits due to upstream man-made interventions are, in some cases, also a driver for a reduced sediment supply to coastal areas (Xue et al., 2009; Yang et al., 2017). Concurrently, erosion, mainly driven by wave action, has stayed the same and is expected to grow due to stormier seas (Masson-Delmotte et al., 2021). This results in sediment starvation, where tidal flats and salt marshes require sediment to prevent them from eroding. This disbalance in sedimentation and erosion leads to volume and elevation decrease of tidal flats and salt marshes (Santinelli & Ronde de, 2012). Elevation decrease in these areas can become problematic since dikes with significant foreshores dissipate incoming wave energy and stabilize the shoreline (Gedan et al., 2011; Möller et al., 2014; Vuik et al., 2019). The reduced sediment supply to tidal flats and salt marshes is furthermore a critical factor limiting their adaptability to sea level rise (Ladd et al., 2019). Moreover, salt marshes have high ecological value, and they have a function in the sequestration of blue carbon (van Belzen et al., 2020). Hence, losing these valuable functions will result in costly interventions to maintain them.

However, the disbalance in sediment dynamics may be restored by integrating coastal engineering solutions on intertidal foreshores that reduce wave energy and limit erosion. Traditionally, hard and impermeable structures, such as seawalls or stones, are used to attenuate waves and prevent erosion (Hamm et al., 2002). Although they fulfil their function as wave-breaker, they often generate adverse effects like loss of biodiversity, scouring in front of the structure, and disturbed sediment dynamics (Fauvelot et al., 2009, 2012; Gracia et al., 2018; Griggs, 2005). This is because the environment in front of a hard structure is exposed to the same or even higher energetic conditions as before the construction. This generates a lot of wave reflection and turbulence and, therefore, a lack of natural gradient from pioneer- to low- and middle salt marsh zone with corresponding rare biodiversity (Lefeuvre et al., 2003; van der Wal et al., 2008) (see Figure 1). These are reasons why there is a growing consensus toward the application of more permeable and biogenic designs. Examples of artificial biogenic structures are brush-filled breakwalls, gabions filled with shells, BESE elements (Biodegradable EcoSystem Engineering Elements) (BESE-Elements, n.d.), and geotextile. The choice of which biogenic structure to use depends on several factors and is site-specific. Still, the modular behaviour of filled gabions makes it a promising method for implementation in field situations. Due to their porousness and more permeable character, they can mitigate wave energy, facilitate sediment deposition, reduce scour, and develop into self-sustaining reefs by offering substrate for shellfish to settle on (Herbert et al., 2018; Walles et al., 2016). However, the assessment of the interaction of waves with more permeable and porous structures is restricted and is considered to be the biggest knowledge gap in describing wave transmission and reflection (Safak et al., 2020).

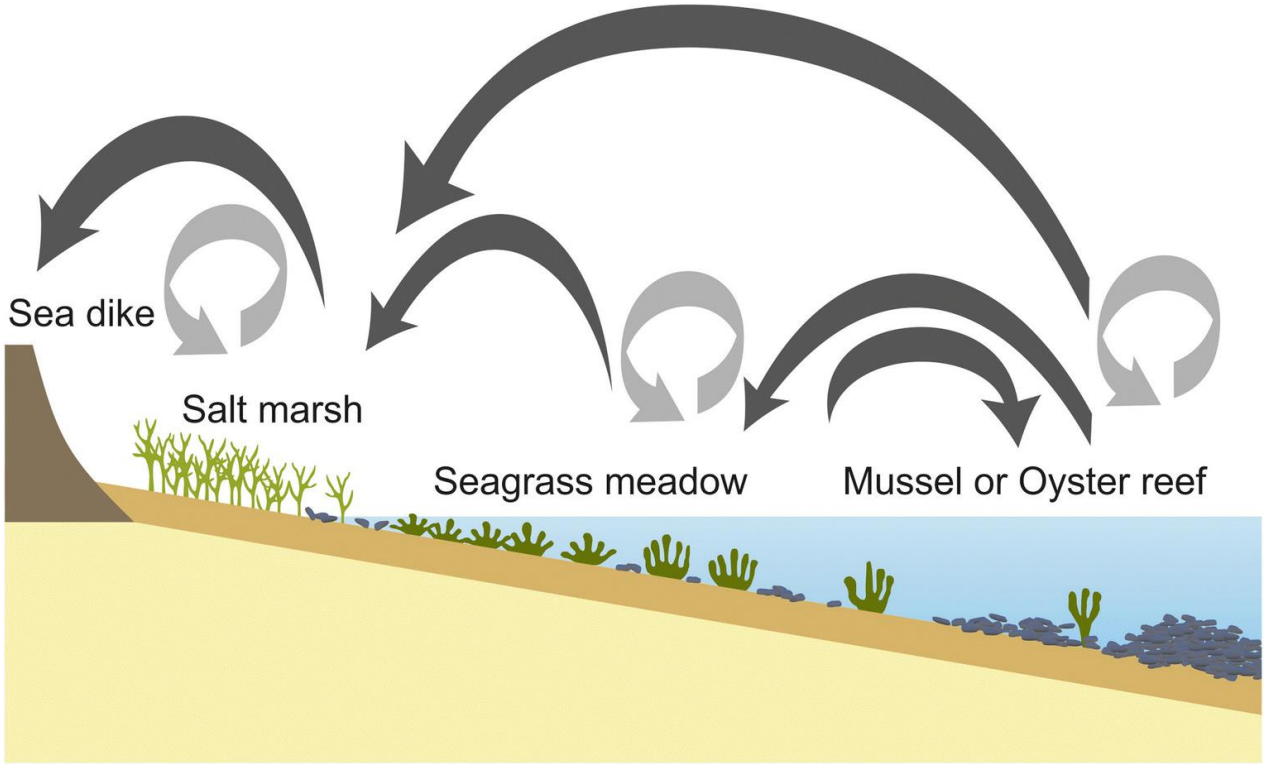

Figure 1. Gradient of a salt marsh ecosystem with ecological engineering in the form of a mussel or oyster reef. The reef stabilizes and protects the coast. Arrows indicate positive interactions. From Schoonees et al. (2019).

1.1 Research question and objectives

The main focus of this empirical research is to gain more insight into the wave attenuation potential and adverse generating effects of four permeable, biogenic materials: loose brushwood, bundled brushwood, empty oyster shells, and empty mussel shells. This will be compared to an impermeable, hard coastal engineering solution in the form of brick stones. The main research question of this study is:

How does wave transformation differ between hard and various biogenic materials in coastal engineering solutions?

To answer this question, four sub-questions have been formulated:

1. *Are there differences in wave attenuation potential between hard and the various biogenic coastal engineering solutions?*
2. *Are there differences in the adverse generating effects of wave reflection and scouring between the hard and various biogenic coastal engineering solutions?*
3. *What is the influence of structure geometry and wave characteristics on wave reflection and attenuation?*
4. *Is there a link between the permeability of the structure and wave attenuation, reflection, and scouring?*

The results will help decision-makers better understand the possibilities of different structures that can be applied on intertidal foreshores to counteract sediment starvation.

1.2 Overview and approach

This study starts with a more detailed comparison of the advantages and disadvantages of hard and biogenic structures in coastal defence schemes. Hereafter, an explanation of the wave transformation process over a wave damping structure is given, which is a function of structure geometry, wave characteristics, and water level. Comprehensive studies will be used to compare existing knowledge on wave transformation of the various materials. Wave energy attenuation, reflection, and bed shear stress will be quantified in an experimental race-track flume at the Royal Institute for Sea Research (NIOZ) in Yerseke. The various materials will be tested in different heights and exposed to an extensive range of near-shore wave characteristics and water levels. Additionally, an experiment will be performed to quantify the permeability using Darcy's law, which can be linked to the different materials' wave energy attenuation, reflection, and scouring potential.

2 Theoretical framework

2.1 Hard and biogenic materials

Coastal engineering solutions are divided into a large variety of categories (Morris et al., 2018). This study categorized them into hard, impermeable and biogenic, permeable structures.

2.1.1 Hard, impermeable structures

The traditional way of offering coastal safety by counteracting erosion is the deployment of hard coastal engineering solutions, like breakwaters, riprap, bulkheads, or groynes (Hamm et al., 2002). Hard coastal engineering solutions usually consist of almost impermeable and non-biogenic material, such as concrete or stones (see Figure 2). They are constructed to dissipate wave energy and withstand extreme environmental conditions. In several densely populated areas, it is still the only alternative (Pranzini, 2018; Rangel-Buitrago et al., 2018). Often, there is no or insufficient space in those areas for nature creation or restoration (Bouma et al., 2014). An example of successful implementation of a hard structure was in The Netherlands, where the construction of stone dams has reduced salt marsh retreat at the Oosterschelde, Terschelling, and Ameland (Teunis & Didderen, 2018; van Loon-Steensma & Slim, 2013). The implementation of hard structures is expected to increase in response to stormier seas and sea-level rise (Masson-Delmotte et al., 2021; Michener et al., 1997). Hard coastal engineering structures, however, can also generate unintended, disadvantageous effects, such as:

1. Changed hydrodynamics. The construction of any offshore structure generates alterations in hydrodynamics and other processes such as water flow, depositional processes, wave regime, and sediment dynamics (Dugan et al., 2012). Hard structures generate increased wave reflection, leading to active erosion or scouring in front of the structure (Irie & Nadoaka, 1985; Pearce et al., 2007). Scouring leads to instability or sinking of the structure and is an important reason for the failure of many coastal engineering solutions (Ranasinghe & Turner, 2006). Moreover, the reflected currents may generate changed sediment dynamics and, therefore, beach reduction or erosion of adjacent coastal areas (Rangel-Buitrago et al., 2018; Schoonees et al., 2019). The negative sediment balance induced by the construction of hard engineering solutions may be mitigated by periodically shore nourishment. This, however, has negative environmental effects at both the extraction and deposition location, such as biota burial, increased turbidity, and sedimentation (Schoonees et al., 2019).
2. Loss or damage of natural landforms and corresponding biodiversity. The sudden transition in hydrodynamic forces caused by the construction of a hard structure often leads to steepening of the slope and hence a lack of natural gradient from the sea to the coast (Masselink et al., 2020). Additionally, ponding of seawater due to poor drainage may lead to a lack of vegetation development. This was observed in the abovementioned example of the stone dam construction at the Oosterschelde (van Belzen et al., 2020).
   Salt marshes are a good example of this, where the pioneer- to low- and middle salt marsh zone includes a large variety of rare biodiversity and connectivity (Dugan et al., 2012; van der Wal et al., 2008).

3. The unnatural visual appearance. The hard structures may also be dangerous for boats, swimmers, and other recreational activities.

Figure 2. Two examples of coastal protection by the integration of hard structures. a) breakwater that stimulates sediment accretion at Colonial National Historic Park, Virginia (Steve Simons, 2012). *b) groin structure along the coast of New Jersey* (NPS photo, n.d.)

2.1.2 Biogenic, permeable structures

Biogenic coastal engineering solutions consist of material of ecological or biological origin. Due to the obtained porousness and more permeable structure, they can mitigate wave energy, facilitate sediment deposition and reduce scouring (Herbert et al., 2018). A distinction is made between natural and artificial biogenic structures. Natural biogenic structures result from natural or biological processes (i.e., oyster reefs, mussel beds, seagrass, or salt marshes). Artificial biogenic structures are man-made (i.e., brush-filled breakwalls, biodegradable geotextile, or BESE elements) (Safak et al., 2020). Temporary materials that facilitate the settlement of shellfish, from which a self-sustained reef can develop, are also seen as artificial structures (i.e., gabions filled with shells, reef balls, or oyster castles) (Safak et al., 2020; Theuerkauf et al., 2015).

2.1.2.1 Brush-filled breakwalls

Brush-filled breakwalls are wooden piles or fences filled with bundles of branches, brush, or tree trunks (see Figure 3). They are widely implemented for land reclamation and to protect salt marshes. Besides their ability to attenuate waves, they also facilitate fine suspended sediment deposition while the erosion of accumulated sediment is hampered (Herbert et al., 2018; Hofstede, 2003). The Netherlands has a long history of using brush-filled breakwalls. They were originally used for land reclamation in Groningen and Friesland. Currently, they are also used on a smaller scale in Zeeland for land reclamation and to protect salt marshes. Brush-filled breakwalls can also be used in combination with other biogenic structures. During a study by Safak et al. (2020), brush-filled breakwalls were used to successfully protect gabions filled with shells. Due to the high wave energy, unprotected gabions were uplifted and pushed back into the adjacent salt marsh.
Another advantage of brush-filled breakwalls is their relatively low construction- and material cost. However, The wood-rotting makes the maintenance of brush-filled breakwalls a labour-intensive process. It includes the reparation of flush holes, piles, wire, and refilling of the wood.

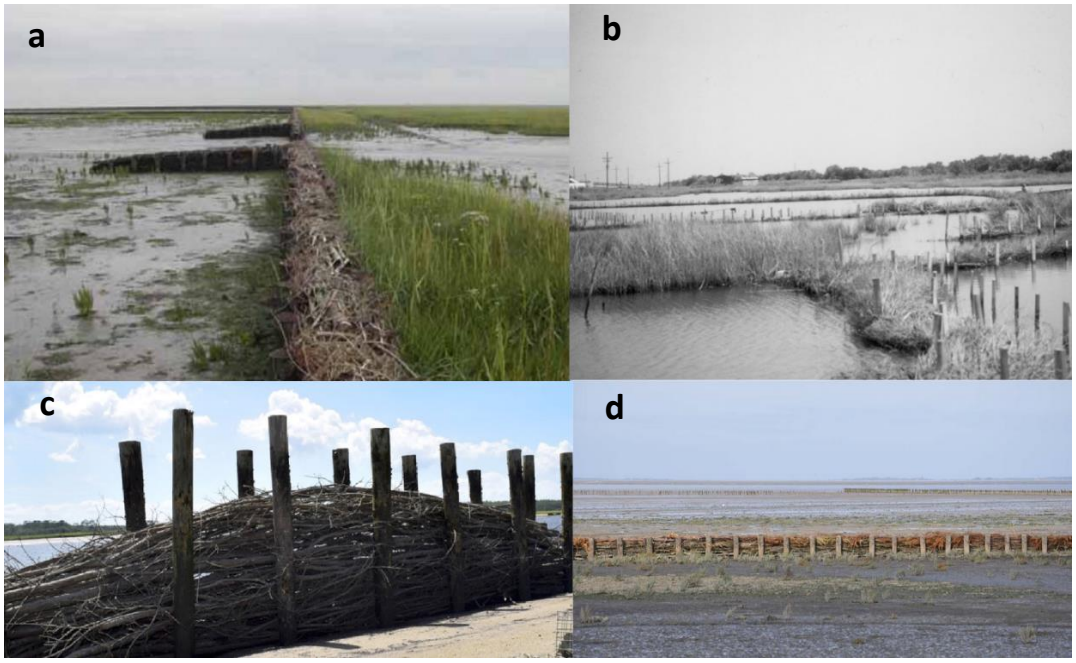

Figure 3. Examples of brush-filled breakwalls. a) Friesland, The Netherlands(van Duin et al., 2007*). b) Louisiana coastal marshes* (Boumans et al., 1997). *c) Ponted Bedra Beach, Florida* (Herbert et al., 2018). *d) Friesland, The Netherlands* (de Leeuw et al., 2018).

2.1.2.2 Oysters and mussels

Oysters and mussels are bivalve shellfish species and are commonly known as ecosystem engineers. They alter their environment in such a way that other species can benefit from it. They are economically valuable because they deliver a lot of important ecosystem services, such as water quality improvement, shoreline stabilization, habitat provision for epibenthic fauna and other fish species, increased biodiversity, and enhanced oyster production (Grabowski et al., 2012; van der Schatte Olivier et al., 2020). Their ability to attenuate wave energy, trap- and stabilize sediment, and to keep up with rising sea level are the main reason why more artificial oyster reefs are proposed in coastal defence schemes (Borsje et al., 2011; Bouma et al., 2014; Morris et al., 2018; Temmerman et al., 2013; Walles et al., 2016). Artificial oyster reefs are implemented and used in different forms and configurations (see Figure 4):

1. Gabions and mats (Figure 4a). Gabions with oysters are cage-shaped structures, usually made from steel wire. An important advantage of gabions is their modularity, making it possible to locate them in different configurations spatially. They can basically be filled with lots of different materials, such as stones, mussels, and oysters. Mussels and oysters are often preferred since they offer substrate for other shellfish to settle on (Walles et al., 2016). This increases friction and consequently wave attenuation.
2. Concrete rings (Figure 4b). Under more extreme environmental circumstances, gabions filled with loose shells are not stable enough to withstand extreme environmental conditions. Chowdhury et al. (2019) used more robust structures in the form of 0.6-meter-high concrete rings to prevent salt marshes on an island near Bangladesh from disappearing. Oysters successfully settled on these structures.
3. Reefballs (Figure 4c). Another type of wave damper that also offers substrate for oysters are reefballs. They can be constructed in different sizes and shapes but generally look like curved balls with holes. They are designed to attract marine life (KOJANSOW et al., 2013; Saleh et al., 2018).

4. Oyster castles (Figure 4d). Oyster castles are prefabricated substrates consisting of a mixture of concrete, limestone gravel, and crushed oyster shell (Theuerkauf et al., 2015). They can also be constructed in different sizes and shapes but generally consist of parapets on top of blocks with a tower-like shape.

*Figure 4. Artificial oyster reefs are used in different forms and configurations. a) gabions filled with empty oyster shells at the Eastern Scheldt, The Netherlands (*Oyster Reefs*, 2009). b) concrete rings used to protect salt marshes at an island of Bangladesh* (Chowdhury et al., 2019). *c) reefballs at Sabah, Malaysia* (Saleh et al., 2018)*). d) oyster castles at cheasapeake bay, North of united states* (Theuerkauf et al., 2015).

2.2 Theory on wave transformation of a wave damping structure

The wave energy balance of a wave which is interacting with a structure in a closed environment and a constant water level is described by the law of conservation of energy (as in Koley et al., 2020; Neelamani & Rajendran, 2001):

(1) $$K_t^2 + K_r^2 + K_l^2 = 1$$

(2) $$K_l = \sqrt{1 - K_r^2 - K_t^2}$$

Part of the incident wave energy will be transmitted through the structure (K_t^2), part of the incident wave energy will be reflected (K_r^2), and part of the incoming wave energy will be dissipated by the structure (K_l^2) (see Figure 5).

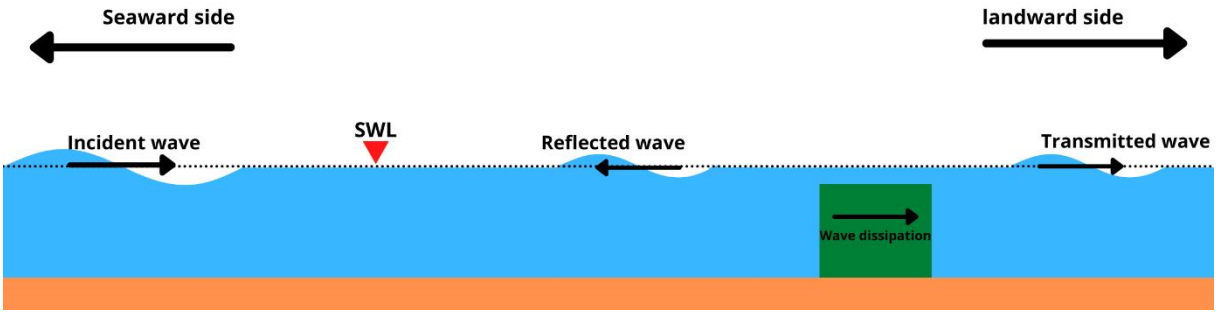

Figure 5. Part of the incident wave energy is reflected, part of the wave energy is transmitted and part of the wave energy is dissipated.

K_t and K_r are, in most empirical studies, described as a function of wave height (Seabrook & Hall, 1998; Srineash & Murali, 2019; van der Meer et al., 2005):

(3) $$K_t = \frac{H_t}{H_0}$$

(4) $$K_r = \frac{H_r}{H_0}$$

Where H_i, H_t and H_r are incident wave height, transmitted wave height, and reflected wave height respectively.

2.2.1 Structure variables and wave characteristics

The hydrodynamic performance of a wave damping structure is a function of the structure geometry and characteristics of the incident waves (Seabrook & Hall, 1998):

(5) $$(K_r, K_t, K_l) = f(h_{s,}, h, d_s, H_0, B, L, n)$$

Where h_s is the height of the wave damping structure, h the water level, d_s the depth of submergence, H_0 the incident wave height, B the width of the wave damping structure, L the wavelength, and n the porosity (see Figure 6).

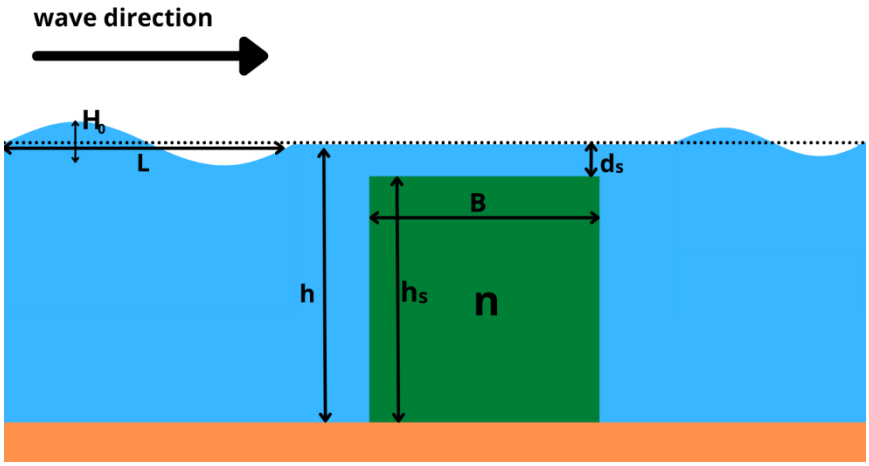

Figure 6. Structure variables and wave characteristics of a wave damping structure

In most empirical studies, some of the parameters of equation (5) are brought in extensive varieties of non-dimensional forms to scale them to field situations and to relate them to processes responsible for wave dissipation by wave damping structures (Seabrook & Hall, 1998; Srineash & Murali, 2019; van der Meer et al., 2005). For example:

(6)

$$(K_r, K_t, K_l) = f\left(\frac{h}{h_s}, \frac{d_s}{H_0}, n\right)$$

The parameters of equations (5) and (6) are discussed in the section below.

2.2.1.1 Structure height (h_s)

The structure height is an important parameter describing wave attenuation and reflection by a wave damping structure. Two ways of expressing the structure height in non-dimensional form are in means of the submergence ratio and the relative submergence.

2.2.1.1.1 Submergence ratio

The submergence ratio is the ratio between the water depth (h) and the structure height (h_s):

(7)

$$SR = \frac{h}{h_s}$$

In intertidal areas, submergence ratios of wave damping structures differ significantly due to varying water levels. A distinction is made between four different conditions: emergent where SR ≤ 1, near-emergent where 1 ≤ SR ≤ 2, transitional submerged 2 ≤ SR ≤ 10, and deeply-submerged where SR > 10 (Augustin et al., 2009). The effects of wave damping structures in microtidal areas (tidal difference < 2m) are less variable over time than in meso- (tidal difference 2-4m) or macrotidal areas (tidal difference >4m). Thus, the relation between submergence ratio and wave attenuation is for decision-makers an important correlation in deciding the height or elevation location of the wave damping structure on the intertidal foreshore.

2.2.1.1.2 Relative submergence

In most literature about submerged wave damping structures, the structure height is expressed as the relative submergence, which is the ratio between the depth of submergence (d_s) and the incident

wave height (H_0) (Blenkinsopp & Chaplin, 2008; Briganti et al., 2003; Seabrook & Hall, 1998; Srineash & Murali, 2019; van der Meer et al., 2005):

(8)
$$RS = \frac{d_s}{H_0}$$

Different analytical studies found clear correlations between relative submergence and wave transmission and described it as the most important parameter affecting wave transmission by submerged wave damping structures (Blenkinsopp & Chaplin, 2008; Briganti et al., 2003; Seabrook & Hall, 1998; Srineash & Murali, 2019; van der Meer et al., 2005). Those studies also indicate that relative submergence is the dominant parameter responsible for breaking the waves.

2.2.1.2 Porosity and material properties

The porosity of the structure is described as the amount of open space within the structure and is closely related to the density and permeability. It is the ratio between the pore volume V_p and the total volume V_t.

(9)
$$n = \frac{V_p}{V_t}$$

Some empirical studies describe the wave transmission of a submerged breakwater to be independent of the porosity of the structure (d'Angremond et al., 1997; Medina et al., 2020; van der Meer et al., 2005). Other studies relate the rock size of a rubble mound breakwater to flow within the structure and, therefore, indirectly to the porosity (Seabrook & Hall, 1998; van der Meer & Daemen, 1994).

Most studies that take the porosity or permeability into account base their essence on the Forchheimer equation, which is an extension of Darcy's law with an additional second-order term that accounts for the resistance of unsteady flow (Engelund, 1953; Safak et al., 2020). Madsen. (1974) derived empirical relations for reflection and transmission coefficient as:

(10)
$$K_t = \frac{1}{1 + \lambda}$$

(11)
$$K_t = \frac{\lambda}{\lambda + 1}$$

Where:

(12)
$$\lambda = \frac{k * B * f_w}{2 * n}$$

In which k the wave number is and n the porosity. f_w is defined as the linearized friction parameter:

(13)

$$f_w = \frac{n}{k * B}\left[-\left(1 - \frac{k * B * a}{2 * \omega}\right) + \sqrt{\left(1 + \frac{k * B * a}{2 * \omega}\right)^2 + \frac{16 * \beta}{3 * \pi} * a_i * \frac{B}{h}}\right]$$

In which ω the angular velocity is. α and β are parameters representing laminar and turbulent resistance of the porous structure respectively. Engelund. (1953) suggested that those parameters are a function of porosity n, and a measure of the particle size (d) in the porous medium. The laminar part is furthermore a function of the fluid viscosity v:

(14)

$$\alpha = \alpha_0 \frac{(1-n)^3}{n^2} * \frac{v}{g * d^2}$$

(15)

$$\beta = \beta_0 * \frac{(1-n)}{n^3} * \frac{1}{d}$$

Engelund. (1953) found out that there's a wide range of α_0 and β_0 values, dependent on material properties such as shape or size distribution. For a more detailed description of the derivation of these equations, the reader is referred to Madsen. (1974).

More specifically, the wave transmission and reflection is, contrary to most described empirical relations in literature, not only a function of structure geometry, wave characteristics, and water levels but also of material characteristics (i.e., stiffness, structure, size distribution, porosity, and permeability) (Safak et al., 2020).

2.2.1.3 Wave properties

Wave transformation is, besides material properties, also a function of wave characteristics. Incident wave height and wave period are important parameters determining wave attenuation.

2.2.1.3.1 Incoming wave height (H_0)

The incident wave height influences wave attenuation significantly, which makes intuitive sense since waves with higher incoming wave heights will be dampened more. The incident wave height is in the majority of studies in literature expressed in the relative submergence (see equation (8)) (Blenkinsopp & Chaplin, 2008; Briganti et al., 2003; Seabrook & Hall, 1998; Srineash & Murali, 2019; van der Meer et al., 2005).

2.2.1.3.2 Wave period (t)

Contradictory to structure geometry and incident wave height, the influence of wave period on attenuation is not fully understood yet (Anderson et al., 2011). One study by Möller et al. (1999) concluded that waves with different wave periods were attenuated equally at a salt marsh in England. Other laboratory studies about wave attenuation by vegetation concluded that shorter-period waves were attenuated more (Bradley & Houser, 2009; Lowe et al., 2007). The wave period can also be linked to wavelength and water depth. This was done by a study of Fonseca & Cahalan. (1992), where they made a distinction between three different conditions: shallow water ($h/L < 0.05$), intermediate water ($0.05 < h/L < 0.5$) and deep water ($h/L > 0.5$). They concluded that the waves in the shallow water regime were attenuated more effectively.

2.2.2 Wave transformation of hard structures

Most empirical relations about wave transformation by structures are based on hard coastal engineering solutions (d'Angremond et al., 1997; Medina et al., 2020; Seabrook & Hall, 1998; van der Meer et al., 2005; van der Meer & Daemen, 1994). Hard structures attenuate wave energy especially by the sudden decrease in water depth that develops. This leads to wave breaking; hence the height of the structure largely determines the amount of wave attenuation (Kamath et al., 2017). Higher structures can attenuate a lot of wave energy, automatically leading to more wave reflection. This confirms that the design of the submerged hard breakwater plays an important role in the wave attenuation process.

2.2.3 Wave transformation of brush-filled breakwalls

Different field studies have been performed on the ability of brush-filled breakwalls to attenuate waves (Boumans et al., 1997; Ellis et al., 2002; Safak et al., 2020). Boumans et al. (1997) investigated the influence of breakwalls filled with Christmas trees on wave characteristics, sedimentation, and vegetation development in two Louisiana coastal marshes. They concluded that the fences reduced wave energy on average by 50% for limited water levels and wave heights. Depth variation was not considered. They also found sediment aggradation rates of an order magnitude higher close to the fences than at the control sites.

Ellis et al. (2002) studied the influence of brush-filled breakwalls to protect levees at the San Joaquin River Delta in California. They showed that brush-filled breakwalls reduced on average 60% of incoming wave energy, with water levels fluctuating around 50 cm. The bundles were completely submerged at high tide, while they completely emerged during low tide. They also concluded that the wave energy attenuation was strongly depth-dependent.

A more recent study from Safak et al. (2020) analyzed the potential of brush-filled breakwalls in reducing boat wake energy at two locations within the Atlantic Intracoastal Waterway in Northeast Florida. As an additional experiment, they investigated the influence of the porosity of the breakwall in reducing incoming wave energy. They concluded that in the design where the branches were bundled and a porosity of 0.7 was maintained, wave energy transmission was on average 53% with a strong depth dependence. In the design where the branches were not bundled, a higher porosity of 0.9 could be obtained. This more porous breakwall transmitted on average 83% of incoming wave energy with a less depth dependency.

The different field studies show that the amount of wave attenuation by brush-filled breakwalls is depth-dependent and largely determined by material properties, such as branch diameter distribution, packing, porosity, and roughness (Herbert et al., 2018). Although a low porosity seems a good property in withstanding extreme environmental conditions, it could also result in breakwalls acting as hard structures, inducing scour and instability (Herbert et al., 2018; Pearce et al., 2007). Flume studies about the wave attenuating potential of brush-filled breakwalls, where the influence of environmental circumstances can be reduced and regulated, are lacking in literature.

2.2.4 Wave transformation of artificial oyster reefs

Different studies have been performed on the ability of oyster structures to attenuate waves (Allen & Webb, 2011; Armono & Hall, 2003; Chowdhury et al., 2019; Manis, 2013). Allen & Webb. (2011) obtained wave transmission values for bags filled with oysters of different dimensions. They found a correlation that was comparable to a relation found by van der Meer et al. (2005) for low crested

hard breakwaters. Wave transmission over those oyster bags increased with increasing submergence ratio.
Manis. (2013) studied the effectiveness of mats filled with oysters to protect the shoreline from boat wakes at three sites in the Mosquito Lagoon in Florida. He showed that 1-year established oyster reefs attenuated over two times more wave energy than newly deployed shells. Wave transmission coefficients also decreased from 0.93 to 0.74. This can be assigned to the average 8.1 cm vertical accretion and 4.06 cm average sedimentation during this one year.
Armono & Hall. (2003) studied wave attenuation over submerged reef balls. They found on average a wave attenuation of 60% for varying wave conditions and water depths up to 0.6m. Also, this study found a relationship between the submergence ratio and transmission coefficient. Wave transmission increased with increasing submergence ratio.
Wave attenuation by concrete rings on an island of Bangladesh was studied by Chowdhury et al. (2019). They found that waves were attenuated almost completely at water levels below the structure's height (0.6 m). Large waves (40-50cm) were still attenuated at water levels above 1m. This in contrast to smaller waves (10-30cm), which were not dissipated anymore for water levels above 1m. They concluded that the concrete rings have a high potential to protect the coast against erosion. The overall effect of the construction of these rings has led to an erosion reduction of 54%.

The different studies show high potential for using oysters as a wave damping material. Their wave attenuation potential can increase over time due to increased friction induced by oyster growth and attachment. Their ability to keep up with sea-level rise makes it furthermore a promising method for protecting salt marshes and tidal flats. However, using hard substrates, such as concrete rings, oyster castles, and reefballs can also result in these structures behaving like hard structures.

2.2.5 Wave transformation of artificial mussel reefs

There is limited knowledge and experience about wave transformation over artificial mussel structures. On a smaller scale, they have similar effects on sediment deposition and currents as oyster beds (Folkard & Gascoigne, 2009; van Leeuwen et al., 2010). However, natural mussel beds are less effective in wave attenuation than natural oyster beds (Borsje et al., 2011).

3 Material and methods

Three different experiments were conducted. The purpose of the first experiment was to determine the intrinsic permeability of the materials by using Darcy's law. In the second experiment, The materials were exposed to short- and long-period waves to quantify their wave attenuation potential and reflection. This also allowed us to find the frequently-used correlation between the relative submergence and the wave energy change (Blenkinsopp & Chaplin, 2008; Briganti et al., 2003; Seabrook & Hall, 1998; Srineash & Murali, 2019; van der Meer et al., 2005). The last experiment was performed to compare the materials in bed shear stress, which is an indicator of the disadvantageous scouring. All data analysis was done in python 3.8.

3.1 Experimental flume

The experiments were conducted in a 17-meter-long, oval-shaped race-track flume at the Royal Netherlands Institute for Sea Research (NIOZ) in Yerseke. The flume has a width and height of 0.6 and 0.4 meters respectively (see Bouma et al. (2014) for a more extensive description of the flume properties). The flume was filled with saline water from the Eastern Scheldt with a temperature of 8.4 degrees. Measurements were performed at the downstream end of the working section, where a 2-meter-long test section with adjustable bottom and transparent walls was present for visual observations (see Figure 7). The test section was flushed to the bottom with a 2-meter-long wooden plate. Waves were generated by a wave paddle with adjustable frequency settings, and currents of different velocities could be generated with a conveyor belt system working as a paddle wheel. A permeable ramp with artificial grass was installed at the end of the working section, which absorbed wave energy and therefore prevented high waves from topping over the edge of the bending part of the flume. Therefore, a small part of the wave energy was reflected to the test section. This effect was excluded by integrating a control run. It furthermore happens in field situations where wave damping structures are applied on the intertidal foreshore in front of a dike.

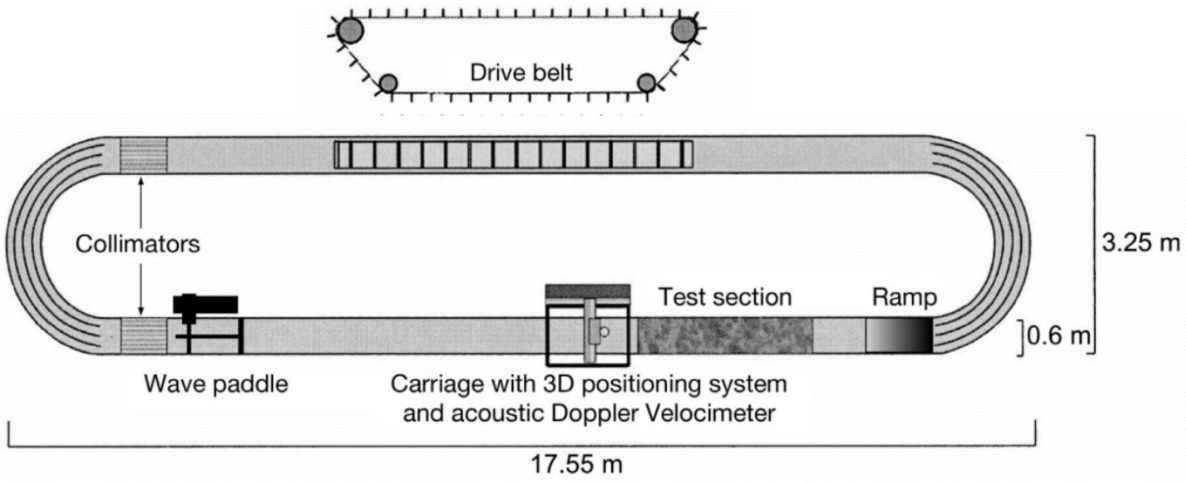

Figure 7. Racetrack flume where the experiments were conducted (adapted from Bouma et al., 2005).

3.2 Materials

Four duplicate steel gabions were filled with different hard and biogenic materials. All gabions had a mesh size, length, and width of 2.5, 57.5, and 57.5 cm respectively. This relatively small mesh size was chosen to prevent small mussels from spilling out during the experiments. The four duplicates

differed in height: 10, 20, 30, and 40 cm, which allowed us to generate different submergence ratios (see 3.3.2.1). The gabions were filled with the following hard and biogenic materials (see also appendix 8.1 for a more extensive description of material properties):

1. Bricks. For the hard structure, limestone bricks with the size of 21 by 10 by 5 cm were used (Figure 8a). The remaining empty spaces were filled up with smaller brick pieces. In this way, an almost impermeable structure could be established.
2. Loose brushwood. Willow branches were cut to a length smaller than the gabion width, making them fit straight in the gabion (57.5 cm, see Figure 8b). This was positioned perpendicular to the wave propagation direction in the flume. The branch diameter lies between 1.1 and 3.3 cm, with an average of 1.8 cm (n=20). This is slightly lower than the wood diameters used in previous experiments on wave attenuation by brushwood(Herbert et al., 2018; Safak et al., 2020).
3. Bundled willow branches. The multifaceted nature of using willow branches to attenuate waves makes it a material that can be tested in several configurations. The wave attenuation will depend on material properties like branch diameter, size distribution, and way of packing or bundling. In most field situations and experiments, the willow branches are bundled (Ellis et al., 2002; Herbert et al., 2018; Safak et al., 2020). For this reason, a second configuration of the willow wood branches is tested in the flume. The same branches are tested in another configuration, bundled in 15 branches with elastic tie tubes (diameter 3 mm) (see Figure 8c).
4. Empty oyster shells. The empty oyster shells used for the experiments were a waste product of a fish conservation company (see Figure 8d). This makes it a sustainable and cheap way of reusing this material for larger field applications. Different types of shells were used; some of them were still closed. Their shell length differed from 7.0 to 16.0 cm, with an average of 11.0 cm (n=20). Their shell width, measured at the widest part, ranged between 4 and 10 cm, with an average of 6.3 cm (n=20).
5. Empty mussel shells. The empty mussel shells were also a waste product of the same fish conservation company (see Figure 8e). Their size distribution range was narrower than the oyster shells. Their shell length ranged from 5.0 to 6.0 cm, with an average of 5.5 cm (n=20). Their shell width, measured at the widest part, ranged between 1.7 and 2.9 cm, with an average of 2.3 cm (n=20). Some of the smaller shells were spilt out of the gabion during the experiments. This is not influencing the results since the run time of the experiments was low, and refilling was possible between the experiments.

Figure 8. Five different materials were tested in the flume. a) brickstones. b) loose brushwood. c) bundled brushwood. d) oysters. e) mussels

3.3 Set-up and analysis

3.3.1 Experiment 1: permeability

The permeability of small-grained structures is obtained by using Darcy's law (Darcy, 1856). Darcy's law describes laminar flow through a porous medium. According to this law, the discharge rate (q in m s^{-1}) is a function of the intrinsic permeability of the medium (k in m^2), the viscosity of the fluid (μ in Pa s), and the pressure gradient (dp/dx in Pa m^{-1}). It is described as:

(16)

$$q = \frac{k}{\mu} * \frac{dp}{dx}$$

More specifically, a pressure gradient will arise when viscous fluid flows through a porous medium (see Figure 9). This pressure gradient is a function of intrinsic permeability. An important implication is that Darcy's law is only valid under laminar flow and is generally applied to sediments. Flow through the larger-sized materials of this experiment rather generates turbulence, which will give an offset. In our experiments, we assume that this offset is equal between the materials, making comparison possible.

Figure 9. A pressure gradient arises when a viscous fluid flows through a porous medium.

3.3.1.1 Set-up

The water level of the flume was set to 22 cm. Pressure differences before and after the structure were measured with pressure sensors. Water flow was generated by the conveyor belt system working as a paddle wheel. This system could generate different flow velocities by adjusting the number of rounds per minute (RPM). A calibration was carried out by manually increasing the amount of RPM in the flume without any structure from 100 to 700 with steps of 100. At each step, the horizontal water velocity was continuously measured for 300 seconds with an ADV (Nortek AS© Vectrino Field Probe) positioned 5 cm under the water surface with a sampling frequency of 200 Hertz. After filtering out the measurement points with a beam correlation <= 80, a linear interpolation was applied to convert flow velocity in RPM to m s^{-1} (see appendix 8.4.1).

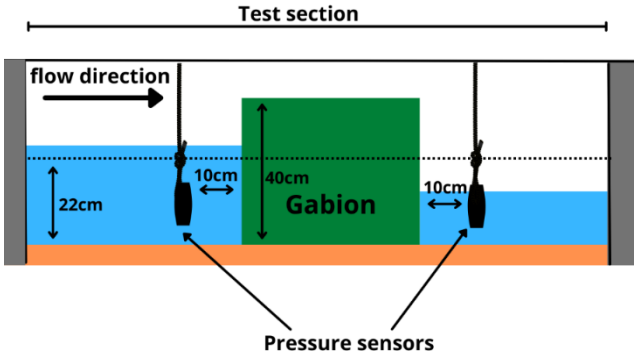

Figure 10. Set up of the permeability measurements.

After the calibration, the gabion of 40 cm height was filled with every single material and positioned in the test section of the flume. Pressure differences were measured with pressure sensors 10 cm before and 10 cm after the structure for 100 seconds with a frequency of 100 Hertz (see Figure 10). Permeability was determined for three different water flow velocities: 150, 300, and 450 RPM.

3.3.1.2 Analysis

The pressure differences were used to calculate intrinsic permeability (m^2) using equation *(16)*, where q the flow velocity of the water is (m s^{-1}) and μ the viscosity of seawater (0.00145 Pa s).

3.3.2 Experiment 2. Wave attenuation and reflection

3.3.2.1 Set-up

Wave attenuation and reflection experiments were carried out on water levels of 22 and 30 cm. In this way, seven different submergence ratios (SR) were generated (see Table 1).

Both emerged (SR < 1) and submerged situations (SR > 1) conditions were mimicked, which is also realistic for intertidal areas where water level fluctuates throughout the day.

Table 1. Overview of the different water levels, structure heights and corresponding submergence ratios

Water level (cm)	Gabion height (cm)	SR (-)
22	10	2.2
22	20	1.1
22	30	0.73
30	10	3.0
30	20	1.5
30	30	1.0
30	40	0.75

For each material, two gabions of the same dimensions were filled up to equal weights (appendix 8.1). In the case of the two willow wood tests, the gabions were filled with ~ the same number of branches. The gabions were positioned 32 cm apart in the test section of the flume. Each pair of gabions were exposed to four different wave conditions (wave period = 2.0, 2.6, 3.4, and 5.1 s) by adjusting the frequency settings of the wave paddle. A distinction is made between short-period waves (t < 3.0 s) and long-period waves (t = 3.0 and 8.0 s) (Rupprecht et al., 2017). Short-period waves are common in intertidal areas, while long-period waves are found during storm surges (Wolf & Flather, 2005).

Wave parameters were measured with three pressure sensors which measure pressure changes in Voltage with a frequency of 100 Hertz. The sensors were calibrated every day since day-to-day air pressure differed significantly. This was done by lowering them into a cylindrical glass tube containing measuring tape. Pressure values were read from the monitor at five different depths. Linear regression was applied to convert Voltage units to centimetres.

The pressure sensors were attached to the wall of the flume at a water depth of ~ 5cm. The incident and reflected wave parameters were obtained from a sensor 16 cm in front of the structure. One sensor measured the wave parameters after the first structure, and the last sensor measured the wave characteristics after the second structure. See Figure 11.

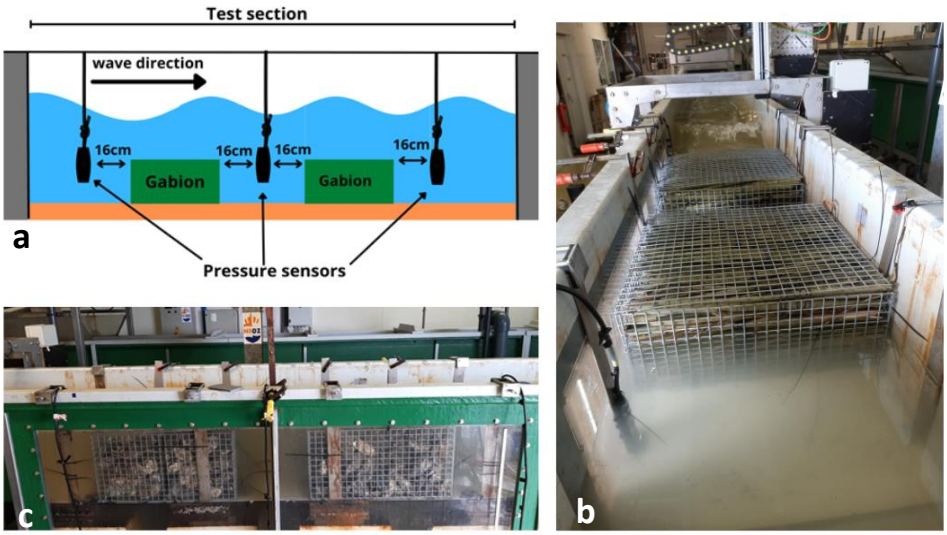

Figure 11. Wave attenuation and reflection set-up.

3.3.2.2 **Analysis**

Quantifying wave properties directly from the time domain was difficult due to the wave reflection induced by the first structure. That's why the datasets of the different runs were transformed into the frequency domain using a Fast Fourier Transform (Welch, 1967). This allowed the calculation of a power spectrum. From this power spectrum, the peak frequency of the waves was determined. The spectral significant wave height at the tree indicated positions in Figure 11a was calculated as:

(17)

$$H_s = \sum_{n=1}^{N} 4 * \sqrt{S(f_n) * \Delta f}$$

In which $S(f_n)$ the energy spectral density is ($cm^2\ Hz^{-2}$), Δf the frequency bandwidth of the spectrum and N the total number of measurements.

The wave energy change was calculated as the difference in spectral significant wave height between the run with structure and the control run, relative to the spectral significant wave height of the control run:

(3)

$$Wave\ energy\ change\ (\%) = \frac{H_{s,x,structure} - H_{s,x,control}}{H_{s,x,control}} * 100$$

This was done for the three positions (x) (see Figure 11a). A wave energy change > 0 would mean a boosting of wave energy compared to the control, while a wave energy change < 0 would indicate damping of wave energy compared to the control run.

3.3.3 Experiment 3. Scouring potential

3.3.3.1 Set-up

The water level of the flume for this experiment was set to 22 cm. The gabion of 30 cm was positioned in the test section of the flume in which the wave paddle generated waves with a wave period of 2.7 seconds and spectral incident wave heights of 8.6 cm. Water flow velocity in x, y, and z-direction was continuously measured with an Acoustic Doppler Velocity meter (Nortek AS© Vectrino Field Probe, ADV), functioning in a 3D positioning system. Where the x-direction is defined as the wave propagation direction, the y-direction is the direction across the flume, and the z-direction is the vertical. The ADV was positioned with its beam 5 cm above the bottom to measure near-bottom flow velocities for 200 seconds with a frequency of 200 Hz. This was done for four positions in front of the structure: 5, 25, 45 and 65 cm to see how far the spatially extended effects of the induced turbulence reach and might affect scouring in the proximity of the structures (see Figure 12).

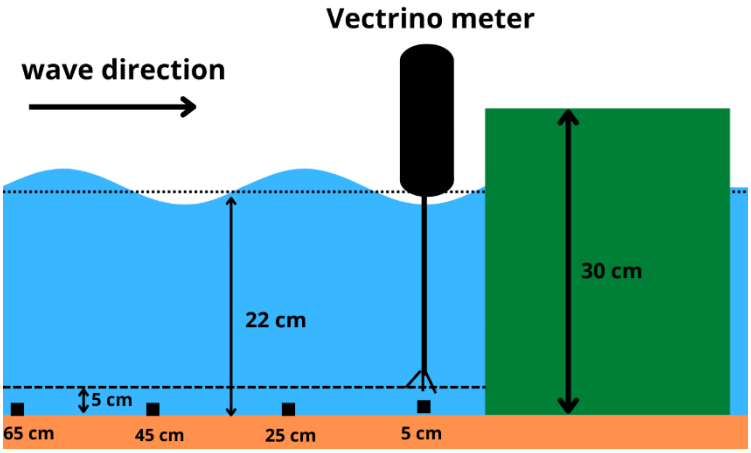

Figure 12. Set-up for the experiments for determination of bed shear stress. Bed shear stress was calculated just abovethe bed (5cm) at five different positions before the structure (5, 25, 45 and 65 cm).

3.3.3.2 Analysis

A 5th order Butterworth low pass filter of 12 Hz was applied to the x, y, and z velocity signal to filter out the part of the spectrum that was dominated by noise. Hereafter, a high pass filter of 4 Hz was applied to separate the wave signal from the turbulence signal (Stapleton & Huntley, 1995). The turbulent kinetic energy was calculated from this turbulent signal as:

(18)

$$TKE = \frac{1}{2} * \rho * (\overline{(u')^2} + \overline{(v')^2} + \overline{(w')^2})$$

Where ρ the density of seawater is (1024 kg m^{-3}). $\overline{(u')^2}$, $\overline{(v')^2}$ and $\overline{(w')^2}$ (m^2 s^{-2}) are the square of the standard deviation in the x, y, and z-direction, respectively. The near-bottom bed shear stress is then proportional to the turbulent kinetic energy (Soulsby, 1983):

(19)

$$\tau = 0.19 * TKE$$

The bed shear stress is an indicator for scouring (Maclean, 1991).

4 Results

4.1 Permeability

The hard structure has the lowest permeability for all three flow velocities (see Figure 13). Furthermore, the configuration where the brushwood was bundled shows for all tests the highest permeability. Personal, visual observation confirms that water flowed quite easily through these bundles of brushwood.
Differences in permeability between the other three materials are clearest observed in the tests performed at lower flow velocities, where the mussels have the second-highest permeability after the hard structure. Hereafter, the loose brush structure and the oysters.

For comparison, the intrinsic permeability of gravel ranges in laminar conditions between 10^{-10} and 10^{-7} m^2 (Jasim et al., 2019).

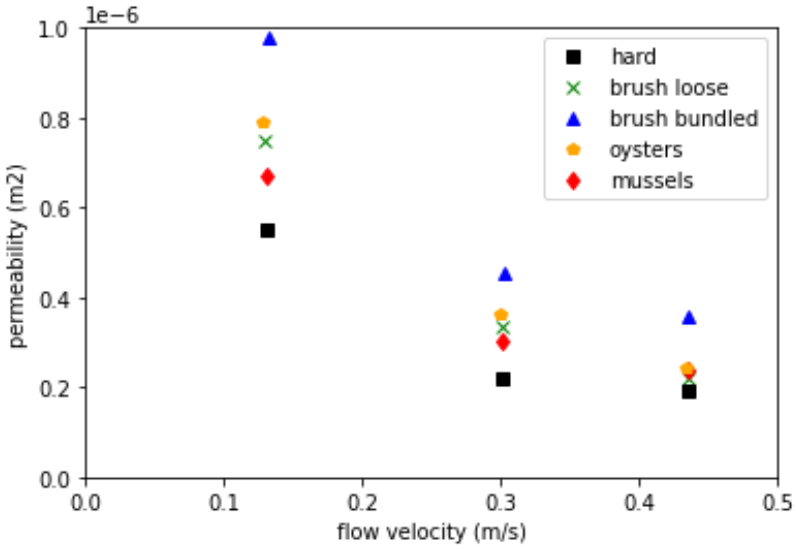

Figure 13. Intrinisic permeability determined for three different flow velocities.

4.2 Wave attenuation and reflection for short-period waves

4.2.1.1 Wave reflection in front of the structure (position 1)

There is in general boosting of wave energy observed for incident short-period waves at the position before the structure (fig.Figure 14aFigure 14dFigure 14g, and Figure 14j). This boosting is a result of wave reflection by the first structure. Furthermore, wave boosting increases with decreasing submergence ratio.

Looking at the differences between the materials, we observe that boosting at low submergence ratios (0.73, 0.75, 1.0, 1.1, and 1.5) is highest for the hard structure. This difference can reach up to 46.2 % for the emerged structure with a submergence ratio of 0.73 (figFigure 14a).

The tests of the gabions with high submergence ratios (2.2 and 3.0) show a maximum range of wave energy change between the materials of only 12.8%. Wave energy-boosting becomes less dependent on material choice for higher submergence ratios.

Moreover, it is remarkable that the mussels at submergence ratios 1.0 and 1.1 generate the lowest boosting of all materials, in general even less than the mussel tests performed at lower submergence ratios. Lower submergence ratios do not always generate more boosting.

Differences between the two configurations of brushwood are small, but bundled branches seem to have a slightly higher boosting of wave energy than the configuration with loose branches.

4.2.1.2 Wave attenuation behind the first structure (position 2)

There is in general damping of wave energy observed for short-period waves at position 2 (fig.Figure 14b, Figure 14e, Figure 14h, and Figure 14k). This damping is a result of wave energy attenuation of the first structure. In these graphs, we also see that wave damping increases with decreasing submergence ratio.

Looking at the differences between the materials, it is seen that the hard structure does not attenuate waves best for low submergence ratios. Instead, damping at low submergence ratios (0.73, 0.75, and 1.0) is highest for the gabions filled with mussels. Personal observations during the experiment reveal that the mussels do not overtop but absorb the waves.

Differences between the other materials are small and remarkable results are inconsistent between the test performed at t = 2.0 and 2.6 s.

4.2.1.3 Wave attenuation behind the second structure (position 3)

For all measurements performed at position 3, wave energy damping was observed (fig.Figure 14c, Figure 14f, Figure 14i, and Figure 14l). This damping is caused by the wave energy attenuation of both structures.

The damping at this position is compared to position 2 especially higher for high submergence ratios. It seems that the emerged structures (low submergence ratio) attenuated most of the wave energy at position 2 already.

The differences between the materials per submergence ratio also lie within a range of a maximum 25%.

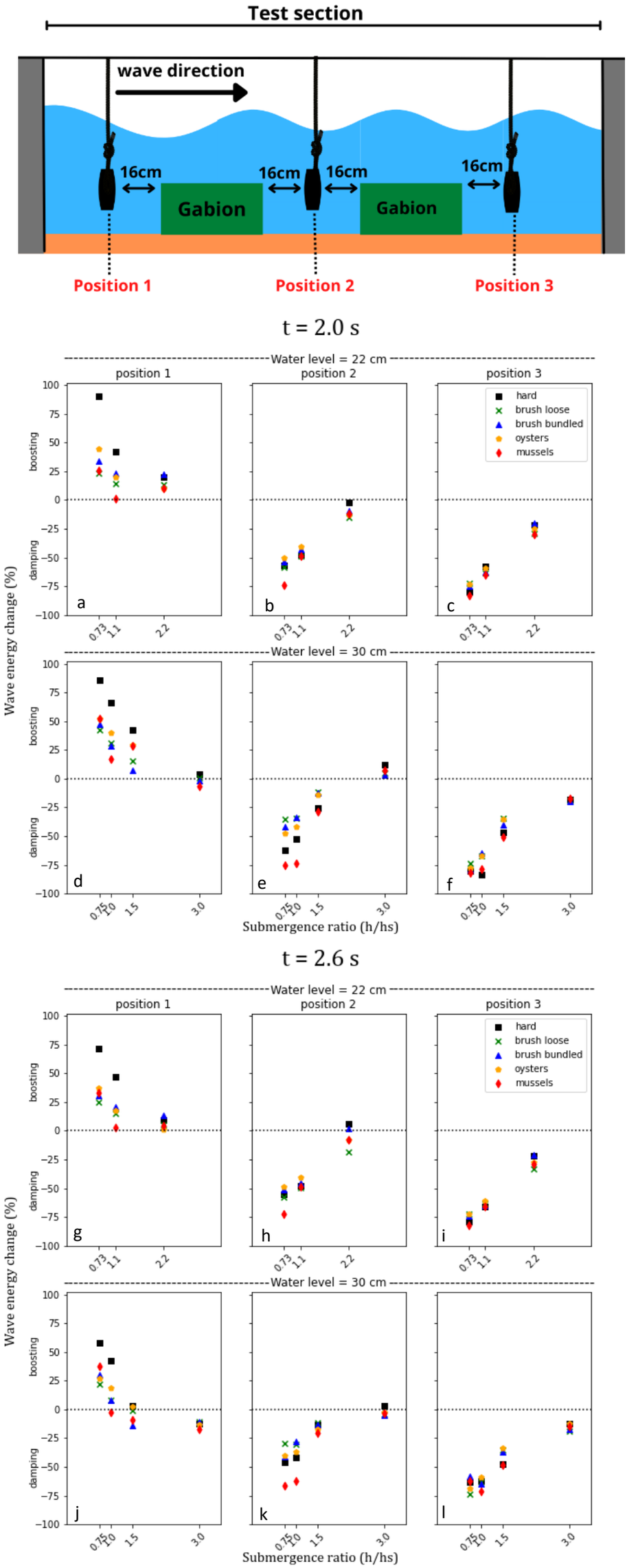

Figure 14. Wave energy change compared to the control run at the three indicated positions for different submergence ratios for short wave periods. a. position = 1, t= 2.0 s, h = 22 cm, b. position = 2, t = 2.0 s, h = 22cm, c. position = 3, t = 2.0 s, h = 22 cm, d. position = 1, t = 2.0 s, h = 30 cm, e. position = 2, t = 2.0 s, h = 30 cm, f. position = 3, t = 2.0 s, h = 30 cm, g. position = 1, t = 2.6s, h = 22 cm, h. position = 2, t = 2.6 s, h = 22 cm, i. position = 3, t = 2.6 s, h = 22 cm, j. position = 1, t = 2.6 s, h = 30 cm, k. position = 2, t = 2.6 s, h = 30 cm, l. position = 3, t = 2.6 s, h = 30 cm.

4.3 Wave attenuation and reflection for long-period waves

4.3.1.1 Wave reflection in front of the structure (position 1)

We also observe in the tests for long-wave periods that the hard structure induces the highest boosting for all tests performed with low submergence ratios (0.73, 0.75, 1.0, and 1.1). The biggest outlier is at a submergence ratio of 0.73 in fig.Figure 15g. Here, a boosting of the hard structure of 179.8% compared to the control run is observed. This boosting of more than 100% is not an exception for the test performed with a wave period of 5.1 seconds and is also observed for the other materials (see fig.Figure 15j). This is because the test of 5.1 seconds generated incident wave heights of only 5.1 and 6.1 cm for water levels of 22 and 30 cm, respectively, making it more likely for the spectral significant wave height to increase more than 100 % at this position. These small incident wave heights are also the reason for the relatively large spread between the materials (fig. Figure 15g andFigure 15j).

4.3.1.2 Wave attenuation behind the first structure (position 2)

At position 2 (fig.Figure 15bFigure 15eFigure 15h, and 15k), a damping of wave energy is expected compared to the control run. This is, however, in general not observed. The correlation with submergence ratio is also less explicit compared to the test performed with shorter-wave periods.

Looking at the differences between the materials, the same finding as the test performed with short-wave periods are observed, where the mussels are attenuating waves best at submergence ratios of 0.73, 0.75, and 1.0 for both water levels (see fig. Figure 15b,Figure 15e, and Figure 15k).

Another remarkable finding is the lower damping of the hard structure at a submergence ratio of 0.73 in figureFigure 15b. Differences between the two configurations of brushwood are small, and oysters also do not generate large differences compared to the other materials.

4.3.1.3 Wave attenuation behind the second structure (position 3)

At position 3 (Figure 15c, Figure 15f, Figure 15I, and Figure 15l), a damping of wave energy is observed for all tests, indicating that the presence of two structures causes a decrease in wave energy compared to the control run. Differences between the materials are small.

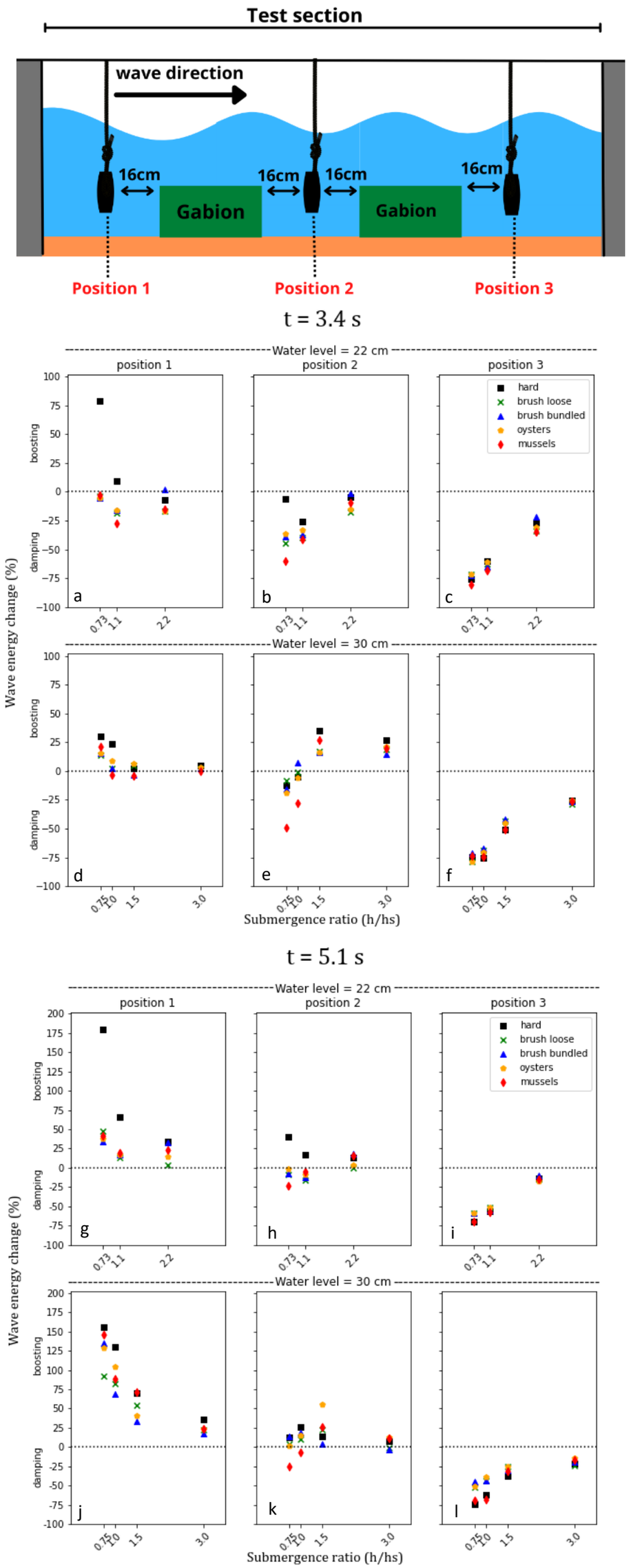

Figure 15. Wave energy change compared to the control run at the three indicated positions for different submergence ratios for long wave periods. Be aware of the different y-axis for the graphs at t = 5.1 s. a. position = 1, t = 3.4 s, h = 22 cm, b. position = 2, t = 3.4 s, h = 22cm, c. position = 3, t = 3.4 s, h = 22 cm, d. position = 1, t = 3.4 s, h = 30 cm, e. position = 2, t = 3.4 s, h = 30 cm, f. position = 3, t = 3.4 s, h = 30 cm, g. position = 1, t = 5.1 s, h = 22 cm, h. position = 2, t = 5.1 s, h = 22 cm, i. position = 3, t = 5.1 s, h = 22 cm, j. position = 1, t = 5.1 s, h = 30 cm, k. position = 2, t = 5.1 s, h = 30 cm, l. position = 3, t = 5.1 s, h = 30 cm.

4.4 Relative submergence

The correlation between the relative submergence and the wave energy boosting/damping at the position before and after the first structure has a large spread and therefore a low R^2 when plotting a linear regression (see Figure 16). The tests of 5.1 s generated large outliers particularly.

However, it was also observed that some findings were consistent in all tests. For example, the higher boosting in front of the hard structure for low submergence ratios. It is, therefore, seen that at this position the slope of the hard structure is almost three times as high as the other materials (see Figure 16a). Differences between the other materials at other positions are small.

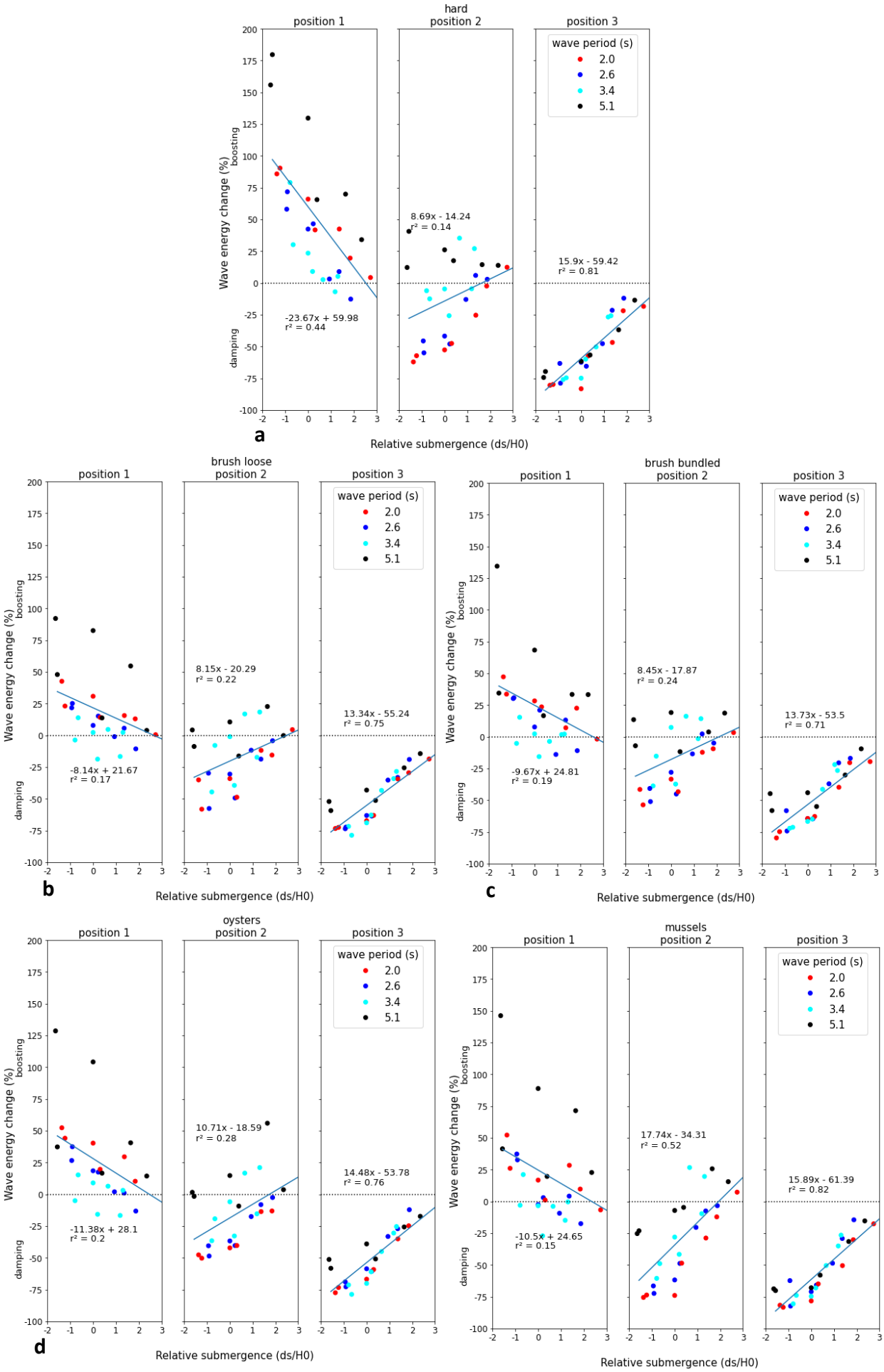

Figure 16. Correlation between the relative submergence (d_s/H_0) and the wave energy change for the three different positions. a) hard, b) brush loose, c) brush bundled, d) oysters, e) mussels.

4.5 Scouring Potential

At 5 cm before the structure, the largest differences are found in bed shear stress, where the hard structure generates the highest from all materials (See Figure 17). From the biogenic materials, the oysters create the highest bed shear stress at this position. After that, the two configurations brushwood and the mussels generate an even lower bed shear stress than the control run, which is difficult to declare. At 65 and 45 cm before the structure, the presence of the structure is hardly measured in means of bed-shear stress.

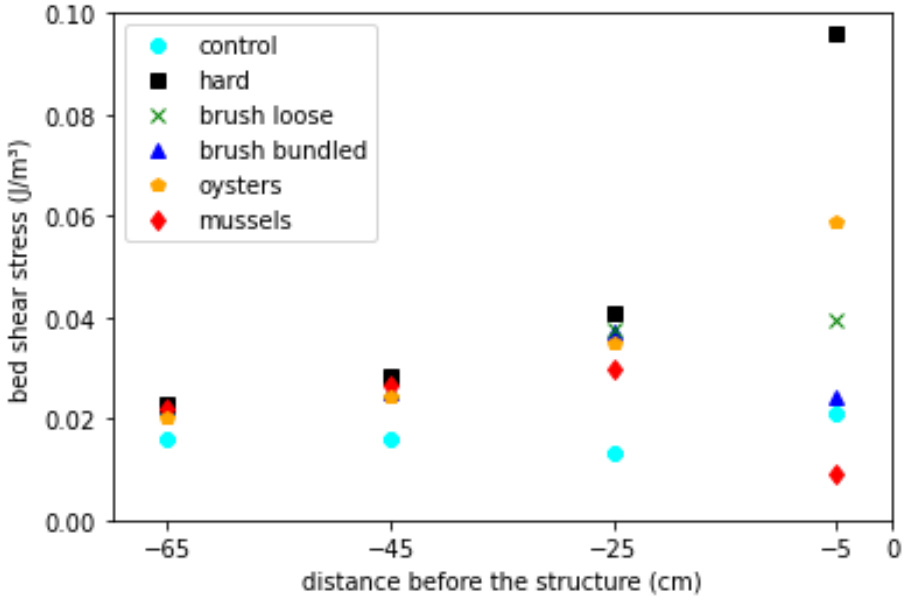

Figure 17. Bed shear stress was measured 5 cm above the bed at 4 different positions before the structure (5, 25, 45 and 65 cm). The control run is the run without a structure.

5 Discussion

This flume study quantified and compared the wave attenuation potential between a hard, impermeable structure and various biogenic, permeable structures. The results show that the hard structure did not attenuate more wave energy than the various biogenic structures. It was even observed that gabions filled with mussels attenuate wave energy better for low submergence ratios. This can partly be attributed to the minimalization of the overtopping of water.
Another comparison was made regarding the adverse generating effects in the structure's proximity. Those effects of wave reflection and bed shear stress were higher for the hard structure than the various biogenic structures, especially for emerged situations.
In addition, the importance of structure geometry and wave characteristics was explored. The correlation with the relative submergence showed that the influence of wave characteristics is crucial in describing wave attenuation and reflection.

5.1 Negative effects of hard, impermeable structure

The results of this experimental study confirm why there is a growing consensus toward the implementation of more permeable instead of hard materials in coastal defence schemes to protect salt marshes and tidal flats from eroding (Borsje et al., 2011; Bouma et al., 2014; Morris et al., 2018; Temmerman et al., 2013; Walles et al., 2016). The main reason for this widespread agreement among researchers was the generation of unintended, disadvantageous effects like wave reflection and scouring in front of a hard structure, which leads to instability and often even failure (Ranasinghe & Turner, 2006). This study confirms that these adverse generating effects are more pronounced for emerged hard structures than the various biogenic structures. Simultaneously, the wave attenuation potential of the hard structure did not show remarkable differences compared to the various biogenic structures. Allen & Webb. (2011) obtained a similar result for a flume experiment about the wave transmission of oyster-filled bags of different dimensions. They found a correlation that was comparable to a relation found by van der Meer et al. (2005) for low crested hard breakwaters.

5.2 Comparison with previous studies

Furthermore, this study is to the best authors' knowledge the only research where a comparison is made between hard and various biogenic materials in means of wave attenuation and reflection under controlled and similar hydrodynamical conditions. Using artificial mussel structures in coastal defence schemes is new and little developed. The wave attenuation potential of brush filled breakwalls was only explored in field situations, where water depth dependency was hard to consider (Boumans et al., 1997; Ellis et al., 2002; Safak et al., 2020). Wave attenuation of oyster shells in coastal defence has mainly been studied using hard substrates, such as concrete rings or reef balls (Armono & Hall, 2003; Chowdhury et al., 2019). Comparing these studies is nearly impossible due to differences in hydrodynamic conditions, structure geometry, and other site-specific parameters. Small differences in, for example, wave characteristics generate already notable differences in means of wave attenuation and reflection.

Moreover, the majority of those earlier mentioned studies only focus on wave attenuation potential and not on the adverse generating effects that might occur in the vicinity of these structures. The

quantification of these adverse generating effects in means of wave energy-boosting and bed shear stress is to the best authors' knowledge also unique in this study.

Furthermore, the influence of the incident wave period on wave transformation was not fully understood yet (Anderson et al., 2011). Möller et al. (1999) concluded that waves of different wave periods were attenuated equally at a salt marsh in England. Our experiments showed that short-period waves were already attenuated after the first structure, while the long-period waves were only attenuated after the second structure. This would indicate that long-period waves are more difficult to attenuate, as also concluded by Bradley & Houser. (2009) and Lowe et al. (2007).

5.3 Limitations

It also became evident that this topic has a multifaceted nature that impacts results, considering:

- Material size. Branch diameter, shell size, shell size distribution, and roughness are all parameters that would influence the performance of a wave dampening structure.
- Way of packing/bundling. Branches of brushwood can be bundled in different configurations and positioned in different directions relative to the wave propagation direction. Furthermore, shells can be compressed or packed together, making the establishment of other shellfish feasible. However, compressed shell structures could also behave as hard structures inducing wave reflection and scouring. In our experiments, wave action led to the rearranging of the material, which was especially evident for mussels. This could also be one of the reasons why mussels attenuated waves best.
- Breaking of the material. Mussel shells were breaking and therefore leaking due to wave action. This was not influencing the results since the run time of the experiments was short, and refilling was possible. In field situations, this is, however, not beneficial.

5.4 Recommendations

Overall, the results of this study make a valuable contribution to existing literature showing the benefits of using biogenic instead of hard materials in coastal defence schemes. Therefore, we advocate further investigation of the behaviour of biogenic structures under natural conditions with irregular waves. The performance of a wave damping structure depends on local hydrodynamic and meteorological conditions, making its behaviour site-specific. Furthermore, it is possible to do more direct measurements of scouring and other important processes in field situations, such as sediment trapping or slope steepening. Such experiments would further develop the knowledge and experience of using biogenic structures to protect salt marshes and tidal flats against sediment starvation.

6 Conclusion

This study conducted various measurements regarding the wave attenuation potential, reflection, and bed shear stress of hard and various biogenic materials. The section below describes the most important conclusions concerning the main research question and the four sub-questions.

Are there differences in wave attenuation potential between hard and various biogenic coastal engineering solutions?
The hard structures did not attenuate more wave energy than the various biogenic structures. It was even visually observed and measured that the emerged mussel structure attenuated wave energy best at the position right after the first structure. This effect can partly be attributed to the minimalization of the overtopping of water due to the relatively small material size of the mussels. It can also partly be due to the rather loose way of packing the mussels, as described in the discussion. Differences between the two configurations of brushwood and oysters were generally small, and remarkable findings were inconsistent over the various experiments.

Are there differences in the adverse generating effects of wave reflection and scouring between the hard and various biogenic coastal engineering solutions?
Wave reflection and bed shear stress in the structure's proximity were highest for the emerged, hard structure. Since wave reflection and bed shear stress are indicators and estimators for the unintended, disadvantageous scouring before a structure, it can be concluded that adverse generating effects were more pronounced for the hard structure compared to the various biogenic structures.
It should be noted that the spatially extended effects of turbulence were nearly not measured anymore at a distance of 45 cm before the structure.

What is the influence of structure geometry and wave properties on wave reflection and attenuation?
A linear regression poorly described the correlation between the relative submergence and the wave energy change. This indicates that the influence of wave properties is essential in describing wave attenuation and reflection. Wave attenuation of short-period waves (2.0 and 2.6s) was already measured after the first structure, while wave attenuation of long-period waves (3.4 and 5.1s) was only measured after the second structure. This would indicate that longer-period waves are attenuated less easily.

Is there a link between the permeability of the structure and wave attenuation, reflection, and scouring?
As expected, the highest permeability was found for the hard structure. It was also found that the emerged, hard structure generated the highest wave reflection and bed shear stress. For the other biogenic structures, differences and remarkable findings were inconsistent over the various experiments. For this reason, it was not possible to link permeability with wave attenuation, reflection and bed shear stress for the various biogenic structures.

How does wave transformation differ between hard and various biogenic materials in coastal engineering solutions?

It turned out that wave transformation between hard and the various biogenic materials did not show striking differences in wave attenuation, except slightly for the mussel structure. The differences are most pronounced in the adverse generating effects in front of emerged structures. Wave reflection and near-bottom bed shear stress were notably higher for the hard structure. These effects were only measured for tests with low submergence ratios. At higher submergence ratios, wave transformation becomes independent of material choice. Moreover, in order to describe wave transformation in means of structure geometry (relative submergence), the importance of wave characteristics, such as wave period should be considered.

7 References

Allen, R. J., & Webb, B. M. (2011). Determination of wave transmission coefficients for oyster shell bag breakwaters. *Coastal Engineering Practice - Proceedings of the 2011 Conference on Coastal Engineering Practice*. https://doi.org/10.1061/41190(422)57

Anderson, M., Smith, J., & McKay, S. (2011). Wave dissipation by vegetation. *US Army Corps of Engineers Engineer Research and Development Center: Vicksburg, MS.*, *September*.

Armono, H. D., & Hall, K. R. (2003). Wave transmission on submerged breakwaters made of hollow hemispherical shape artificial reefs. *Proceedings, Annual Conference - Canadian Society for Civil Engineering*, *2003*.

Augustin, L. N., Irish, J. L., & Lynett, P. (2009). Laboratory and numerical studies of wave damping by emergent and near-emergent wetland vegetation. *Coastal Engineering*, *56*(3). https://doi.org/10.1016/j.coastaleng.2008.09.004

BESE-elements. (n.d.). Retrieved June 7, 2022, from https://www.bese-products.com/

Blenkinsopp, C. E., & Chaplin, J. R. (2008). The effect of relative crest submergence on wave breaking over submerged slopes. *Coastal Engineering*, *55*(12). https://doi.org/10.1016/j.coastaleng.2008.03.004

Boersema, M., Stronkhorst, J., Ysebaert, T., van der Werf, J., Bouma, T., Pesch, C., & Vader, P. (2015). *Variantenstudie en monitoring zandsuppletie Roggenplaats*.

Borsje, B. W., van Wesenbeeck, B. K., Dekker, F., Paalvast, P., Bouma, T. J., van Katwijk, M. M., & de Vries, M. B. (2011). How ecological engineering can serve in coastal protection. In *Ecological Engineering* (Vol. 37, Issue 2). https://doi.org/10.1016/j.ecoleng.2010.11.027

Bouma, T. J., van Belzen, J., Balke, T., Zhu, Z., Airoldi, L., Blight, A. J., Davies, A. J., Galvan, C., Hawkins, S. J., Hoggart, S. P. G., Lara, J. L., Losada, I. J., Maza, M., Ondiviela, B., Skov, M. W., Strain, E. M., Thompson, R. C., Yang, S., Zanuttigh, B., … Herman, P. M. J. (2014). Identifying knowledge gaps hampering application of intertidal habitats in coastal protection: Opportunities & steps to take. *Coastal Engineering*, *87*. https://doi.org/10.1016/j.coastaleng.2013.11.014

Boumans, R. M. J., Day, J. W., Kemp, G. P., & Kilgen, K. (1997). The effect of intertidal sediment fences on wetland surface elevation, wave energy and vegetation establishment in two Louisiana coastal marshes. *Ecological Engineering*, *9*(1–2). https://doi.org/10.1016/S0925-8574(97)00028-1

Bradley, K., & Houser, C. (2009). Relative velocity of seagrass blades: Implications for wave attenuation in low-energy environments. *Journal of Geophysical Research: Earth Surface*, *114*(1). https://doi.org/10.1029/2007JF000951

Briganti, R., van Meer, J. der, Buccino, M., & Calabrese, M. (2003). Wave transmission behind low-crested structures. *Coastal Structures 2003 - Proceedings of the Conference*. https://doi.org/10.1061/40733(147)48

Chowdhury, M. S. N., Walles, B., Sharifuzzaman, S., Shahadat Hossain, M., Ysebaert, T., & Smaal, A. C. (2019). Oyster breakwater reefs promote adjacent mudflat stability and salt marsh growth in a

monsoon dominated subtropical coast. *Scientific Reports*, *9*(1). https://doi.org/10.1038/s41598-019-44925-6

d'Angremond, K., van der Meer, J. W., & de Jong, R. J. (1997). Wave transmission at low-crested structures. *Proceedings of the Coastal Engineering Conference*, *2*. https://doi.org/10.1061/9780784402429.187

Darcy, H. (1856). Les fontaines publiques de la ville de Dijon. *Recherche*.

de Leeuw, C., Bakker, C., Baptist, M. J., & Elschot, K. (2018). *Kansen voor Kwelders*.

Dugan, J. E., Airoldi, L., Chapman, M. G., Walker, S. J., & Schlacher, T. (2012). Estuarine and Coastal Structures: Environmental Effects, A Focus on Shore and Nearshore Structures. In *Treatise on Estuarine and Coastal Science* (Vol. 8). https://doi.org/10.1016/B978-0-12-374711-2.00802-0

Ellis, J. T., Sherman, D. J., Bauer, B. O., & Hart, J. (2002). Assessing the Impact of an Organic Restoration Structure on Boat Wake Energy. *Journal of Coastal Research*, *36*. https://doi.org/10.2112/1551-5036-36.sp1.256

Engelund, Frank. (1953). *On the laminar and turbulent flows of ground water through homogeneous sand.* Akademiet for de tekniske videnskaber.

Fauvelot, C., Bertozzi, F., Costantini, F., Airoldi, L., & Abbiati, M. (2009). Lower genetic diversity in the limpet Patella caerulea on urban coastal structures compared to natural rocky habitats. *Marine Biology*, *156*(11). https://doi.org/10.1007/s00227-009-1259-1

Fauvelot, C., Costantini, F., Virgilio, M., & Abbiati, M. (2012). Do artificial structures alter marine invertebrate genetic makeup? *Marine Biology*, *159*(12). https://doi.org/10.1007/s00227-012-2040-4

Folkard, A. M., & Gascoigne, J. C. (2009). Hydrodynamics of discontinuous mussel beds: Laboratory flume simulations. *Journal of Sea Research*, *62*(4). https://doi.org/10.1016/j.seares.2009.06.001

Fonseca, M. S., & Cahalan, J. A. (1992). A preliminary evaluation of wave attenuation by four species of seagrass. *Estuarine, Coastal and Shelf Science*, *35*(6). https://doi.org/10.1016/S0272-7714(05)80039-3

Gedan, K. B., Kirwan, M. L., Wolanski, E., Barbier, E. B., & Silliman, B. R. (2011). The present and future role of coastal wetland vegetation in protecting shorelines: Answering recent challenges to the paradigm. In *Climatic Change* (Vol. 106, Issue 1). https://doi.org/10.1007/s10584-010-0003-7

Grabowski, J. H., Brumbaugh, R. D., Conrad, R. F., Keeler, A. G., Opaluch, J. J., Peterson, C. H., Piehler, M. F., Powers, S. P., & Smyth, A. R. (2012). Economic valuation of ecosystem services provided by oyster reefs. *BioScience*, *62*(10). https://doi.org/10.1525/bio.2012.62.10.10

Gracia, A., Rangel-Buitrago, N., Oakley, J. A., & Williams, A. T. (2018). Use of ecosystems in coastal erosion management. In *Ocean and Coastal Management* (Vol. 156). https://doi.org/10.1016/j.ocecoaman.2017.07.009

Griggs, G. B. (2005). The impacts of coastal armoring. *Shore & Beach*, *73*(1).

Hamm, L., Capobianco, M., Dette, H. H., Lechuga, A., Spanhoff, R., & Stive, M. J. F. (2002). A summary of European experience with shore nourishment. *Coastal Engineering*, *47*(2). https://doi.org/10.1016/S0378-3839(02)00127-8

Herbert, D., Astrom, E., Bersoza, A. C., Batzer, A., McGovern, P., Angelini, C., Wasman, S., Dix, N., & Sheremet, A. (2018). Mitigating erosional effects induced by boat wakes with living shorelines. *Sustainability (Switzerland)*, *10*(2). https://doi.org/10.3390/su10020436

Hofstede, J. L. A. (2003). Integrated management of artificially created salt marshes in the Wadden Sea of Schleswig-Holstein, Germany. *Wetlands Ecology and Management*, *11*(3), 183–194. https://doi.org/10.1023/A:1024248127037

Irie, I., & Nadoaka, K. (1985). LABORATORY REPRODUCTION OF SEABED SCOUR IN FRONT OF BREAKWATERS. *Proceedings of the Coastal Engineering Conference*, *2*. https://doi.org/10.1061/9780872624382.117

Jasim, A., Hemmings, B., Mayer, K., & Scheu, B. (2019). Groundwater flow and volcanic unrest. In *Advances in Volcanology*. https://doi.org/10.1007/11157_2018_33

Kamath, A., Chella, M. A., Bihs, H., & Arntsen, Ø. A. (2017). Energy transfer due to shoaling and decomposition of breaking and non-breaking waves over a submerged bar. *Engineering Applications of Computational Fluid Mechanics*, *11*(1). https://doi.org/10.1080/19942060.2017.1310671

King, S. E., & Lester, J. N. (1995). The value of salt marsh as a sea defence. *Marine Pollution Bulletin*, *30*(3). https://doi.org/10.1016/0025-326X(94)00173-7

KOJANSOW, J., SOMPIE, D., EMOR, D., & B. RONDONUWU, A. (2013). Fish settlement on reefballs artificial reef and natural coral reef at Buyat Bay and surrounding areas, North Sulawesi, Indonesia. *Galaxea, Journal of Coral Reef Studies*, *15*(Supplement). https://doi.org/10.3755/galaxea.15.229

Koley, S., Panduranga, K., Almashan, N., Neelamani, S., & Al-Ragum, A. (2020). Numerical and experimental modeling of water wave interaction with rubble mound offshore porous breakwaters. *Ocean Engineering*, *218*. https://doi.org/10.1016/j.oceaneng.2020.108218

Ladd, C. J. T., Duggan-Edwards, M. F., Bouma, T. J., Pagès, J. F., & Skov, M. W. (2019). Sediment Supply Explains Long-Term and Large-Scale Patterns in Salt Marsh Lateral Expansion and Erosion. *Geophysical Research Letters*, *46*(20). https://doi.org/10.1029/2019GL083315

Lefeuvre, J. C., Laffaille, P., Feunteun, E., Bouchard, V., & Radureau, A. (2003). Biodiversity in salt marshes: From patrimonial value to ecosystem functioning. The case study of the Mont-Saint-Michel bay. In *Comptes Rendus - Biologies* (Vol. 326, Issue SUPPL. 1). https://doi.org/10.1016/s1631-0691(03)00049-0

Lowe, R. J., Falter, J. L., Koseff, J. R., Monismith, S. G., & Atkinson, M. J. (2007). Spectral wave flow attenuation within submerged canopies: Implications for wave energy dissipation. *Journal of Geophysical Research: Oceans*, *112*(5). https://doi.org/10.1029/2006JC003605

Maclean, A. G. (1991). Bed Shear Stress and Scour over Bed-Type River Intake. *Journal of Hydraulic Engineering*, *117*(4). https://doi.org/10.1061/(asce)0733-9429(1991)117:4(436)

Madsen, O. S. (1974). WAVE TRANSMISSION THROUGH POROUS STRUCTURES. *ASCE J Waterw Harbors Coastal Eng Div*, *100*(WW3). https://doi.org/10.1061/awhcar.0000242

Manis, J. E. (2013). Assessing the effectiveness of living shoreline restoration and quantifying wave attenuation in Mosquito Lagoon, Florida. *Electronic Theses and Dissertations*.

Masselink, G., Russell, P., Rennie, A., Brooks, S., & Spencer, T. (2020). The impacts of climate change on coastal geomorphology and coastal erosion relevant to the coastal and marine environment around the UK. *Marine Climate Change Impacts Partnership (MCCIP) Science Review*, *January*.

Masson-Delmotte, V., Panmao, Z., Pirani, A., Connors, S. L., Péan, C., Berger, S., Caud, N., Chen, N., Goldfarb, L., Gomis, M. I., Huang, M., Leitzell, K., Lonnoy, E., Matthews, J. B. R., Maycock, T. K., Waterfield, T., Yelekçi, O., Yu, R., & Zhou, B. (2021). IPCC, 2021: Summary for Policymakers. In *Climate Change 2021: The Physical Science Basis. Contribution of Working Group I to the Sixth Assessment Report of the Intergovernmental Panel on Climate Change*.

Medina, J. R., Gomez-Martin, M. E., Mares-Nasarre, P., Escudero, M., Oderiz, I., Mendoza, E., & Silva, R. (2020). HOMOGENEOUS LOW-CRESTED STRUCTURES FOR BEACH PROTECTION IN CORAL REEF AREAS. *Coastal Engineering Proceedings*, *36v*. https://doi.org/10.9753/icce.v36v.papers.59

Michener, W. K., Blood, E. R., Bildstein, K. L., Brinson, M. M., & Gardner, L. R. (1997). Climate change, hurricanes and tropical storms, and rising sea level in coastal wetlands. In *Ecological Applications* (Vol. 7, Issue 3). https://doi.org/10.1890/1051-0761(1997)007[0770:CCHATS]2.0.CO;2

Möller, I., Kudella, M., Rupprecht, F., Spencer, T., Paul, M., van Wesenbeeck, B. K., Wolters, G., Jensen, K., Bouma, T. J., Miranda-Lange, M., & Schimmels, S. (2014). Wave attenuation over coastal salt marshes under storm surge conditions. *Nature Geoscience*, *7*(10). https://doi.org/10.1038/NGEO2251

Möller, I., Spencer, T., French, J. R., Leggett, D. J., & Dixon, M. (1999). Wave transformation over salt marshes: A field and numerical modelling study from north Norfolk, England. *Estuarine, Coastal and Shelf Science*, *49*(3). https://doi.org/10.1006/ecss.1999.0509

Morris, R. L., Konlechner, T. M., Ghisalberti, M., & Swearer, S. E. (2018). From grey to green: Efficacy of eco-engineering solutions for nature-based coastal defence. In *Global Change Biology* (Vol. 24, Issue 5). https://doi.org/10.1111/gcb.14063

Neelamani, S., & Rajendran, R. (2001). Wave interaction with T-type breakwaters. *Ocean Engineering*, *29*(2). https://doi.org/10.1016/S0029-8018(00)00060-3

NPS photo. (n.d.). *Groins and Jetties*.

Oyster Reefs. (2009). https://www.ecoshape.org/en/pilots/oyster-reefs/

Pearce, A. M. C., Sutherland, J. S., Obhrai, C., Müller, G., Rycroft, D., & Whitehouse, R. J. S. (2007). *SCOUR AT A SEAWALL- FIELD MEASUREMENTS AND LABORATORY MODELLING*. https://doi.org/10.1142/9789812709554_0201

Pranzini, E. (2018). Shore protection in Italy: From hard to soft engineering … and back. In *Ocean and Coastal Management* (Vol. 156). https://doi.org/10.1016/j.ocecoaman.2017.04.018

Ranasinghe, R., & Turner, I. L. (2006). Shoreline response to submerged structures: A review. *Coastal Engineering*, *53*(1). https://doi.org/10.1016/j.coastaleng.2005.08.003

Rangel-Buitrago, N., Williams, A. T., & Anfuso, G. (2018). Hard protection structures as a principal coastal erosion management strategy along the Caribbean coast of Colombia. A chronicle of pitfalls. *Ocean and Coastal Management*, *156*. https://doi.org/10.1016/j.ocecoaman.2017.04.006

Rupprecht, F., Möller, I., Paul, M., Kudella, M., Spencer, T., van Wesenbeeck, B. K., Wolters, G., Jensen, K., Bouma, T. J., Miranda-Lange, M., & Schimmels, S. (2017). Vegetation-wave interactions in salt marshes under storm surge conditions. *Ecological Engineering*, *100*. https://doi.org/10.1016/j.ecoleng.2016.12.030

Safak, I., Angelini, C., Norby, P. L., Dix, N., Roddenberry, A., Herbert, D., Astrom, E., & Sheremet, A. (2020). Wave transmission through living shoreline breakwalls. *Continental Shelf Research*, *211*. https://doi.org/10.1016/j.csr.2020.104268

Saleh, E., Geng, C. N., Kiat, Y. T., & Isnain, I. (2018). Effect of artificial structures on shoreline profile of Selingan Island, Sandakan, Sabah, Malaysia. *Borneo Journal of Marine Science and Aquaculture (BJoMSA)*, *2*. https://doi.org/10.51200/bjomsa.v2i0.1304

Santinelli, G., & Ronde de, J. (2012). *Volume analysis on RTK profiles of the Eastern Scheldt*. https://doi.org/10.13140/RG.2.2.15945.13927

Schoonees, T., Gijón Mancheño, A., Scheres, B., Bouma, T. J., Silva, R., Schlurmann, T., & Schüttrumpf, H. (2019). Hard Structures for Coastal Protection, Towards Greener Designs. *Estuaries and Coasts*, *42*(7). https://doi.org/10.1007/s12237-019-00551-z

Seabrook, S. R., & Hall, K. R. (1998). Wave transmission at submerged rubblemound breakwaters. *Proceedings of the Coastal Engineering Conference*, *2*. https://doi.org/10.1061/9780784404119.150

Soulsby, R. L. (1983). The bottom boundary layer of shelf seas. *Elsevier Oceanography Series*, *35*(C). https://doi.org/10.1016/S0422-9894(08)70503-8

Srineash, V. K., & Murali, K. (2019). Functional performance of modular porous reef breakwaters. *Journal of Hydro-Environment Research*, *27*. https://doi.org/10.1016/j.jher.2019.07.006

Stapleton, K. R., & Huntley, D. A. (1995). Seabed stress determinations using the inertial dissipation method and the turbulent kinetic energy method. *Earth Surface Processes and Landforms*, *20*(9). https://doi.org/10.1002/esp.3290200906

Steve Simons. (2012). *Breakwaters, Headlands, Sills and Reefs*. https://www.nps.gov/articles/breakwaters-headlands-sills-and-reefs.htm

Temmerman, S., Meire, P., Bouma, T. J., Herman, P. M. J., Ysebaert, T., & de Vriend, H. J. (2013). Ecosystem-based coastal defence in the face of global change. In *Nature* (Vol. 504, Issue 7478). https://doi.org/10.1038/nature12859

Teunis, M., & Didderen, K. (2018). *Blue Carbon in Nederlandse kwelders: Resultaten van vier kwelders in beheergebieden van Natuurmonumenten*.

Theuerkauf, S. J., Burke, R. P., & Lipcius, R. N. (2015). Settlement, growth, and survival of eastern oysters on alternative reef substrates. *Journal of Shellfish Research*, *34*(2). https://doi.org/10.2983/035.034.0205

van Belzen, J., Bouma, T., & Ysebaert, T. (2020). *Blue Carbon in het Verdronken Land van Zuid-Beveland. NIOZ Report 2020-03* (J. van Belzen, T. Bouma, & T. Ysebaert, Eds.; V3 ed.). NIOZ. https://doi.org/doi/10.25850/nioz/7b.b.z

van der Meer, J. W., Briganti, R., Zanuttigh, B., & Wang, B. (2005). Wave transmission and reflection at low-crested structures: Design formulae, oblique wave attack and spectral change. *Coastal Engineering*, *52*(10–11). https://doi.org/10.1016/j.coastaleng.2005.09.005

van der Meer, J. W., & Daemen, I. F. R. (1994). Stability and Wave Transmission at Low-Crested Rubble-Mound Structures. *Journal of Waterway, Port, Coastal, and Ocean Engineering*, *120*(1). https://doi.org/10.1061/(asce)0733-950x(1994)120:1(1)

van der Schatte Olivier, A., Jones, L., Vay, L. le, Christie, M., Wilson, J., & Malham, S. K. (2020). A global review of the ecosystem services provided by bivalve aquaculture. In *Reviews in Aquaculture* (Vol. 12, Issue 1). https://doi.org/10.1111/raq.12301

van der Wal, D., Wielemaker-Van den Dool, A., & Herman, P. M. J. (2008). Spatial patterns, rates and mechanisms of saltmarsh cycles (Westerschelde, The Netherlands). *Estuarine, Coastal and Shelf Science*, *76*(2). https://doi.org/10.1016/j.ecss.2007.07.017

van Duin, W. E., Dijkema, K. S., & Bos, D. (2007). *Cyclisch kwelderwerken Friesland*.

van Leeuwen, B., Augustijn, D. C. M., van Wesenbeeck, B. K., Hulscher, S. J. M. H., & de Vries, M. B. (2010). Modeling the influence of a young mussel bed on fine sediment dynamics on an intertidal flat in the Wadden Sea. *Ecological Engineering*, *36*(2). https://doi.org/10.1016/j.ecoleng.2009.01.002

van Loon-Steensma, J., & Slim, P. (2013). The Impact of Erosion Protection by Stone Dams on Salt-Marsh Vegetation on Two Wadden Sea Barrier Islands. *Journal of Coastal Research*, *29*, 783–796. https://doi.org/10.2307/23486550

Vuik, V., Borsje, B. W., Willemsen, P. W. J. M., & Jonkman, S. N. (2019). Salt marshes for flood risk reduction: Quantifying long-term effectiveness and life-cycle costs. *Ocean and Coastal Management*, *171*. https://doi.org/10.1016/j.ocecoaman.2019.01.010

Walles, B., Troost, K., van den Ende, D., Nieuwhof, S., Smaal, A. C., & Ysebaert, T. (2016). From artificial structures to self-sustaining oyster reefs. *Journal of Sea Research*, *108*. https://doi.org/10.1016/j.seares.2015.11.007

Welch, P. D. (1967). The Use of Fast Fourier Transform for the Estimation of Power Spectra: A Method Based on Time Averaging Over Short, Modified Periodograms. *IEEE Transactions on Audio and Electroacoustics*, *15*(2). https://doi.org/10.1109/TAU.1967.1161901

Wolf, J., & Flather, R. A. (2005). Modelling waves and surges during the 1953 storm. In *Philosophical Transactions of the Royal Society A: Mathematical, Physical and Engineering Sciences* (Vol. 363, Issue 1831). https://doi.org/10.1098/rsta.2005.1572

Xue, Z., Feng, A., Yin, P., & Xia, D. (2009). Coastal erosion induced by human activities: A northwest Bohai sea case study. *Journal of Coastal Research*, *25*(3). https://doi.org/10.2112/07-0959.1

Yang, H. F., Yang, S. L., Xu, K. H., Wu, H., Shi, B. W., Zhu, Q., Zhang, W. X., & Yang, Z. (2017). Erosion potential of the Yangtze Delta under sediment starvation and climate change. *Scientific Reports*, *7*(1). https://doi.org/10.1038/s41598-017-10958-y

8 Appendix

8.1 Material properties

The material properties are given in the table below.

	Material properties							
	Mussels		Oysters		Willow wood	Bricks		
n	Shell length (cm)	Shell width (cm)	Shell length (cm)	Shell width (cm)	Diameter (cm)	Length (cm)	Width (cm)	Height (cm)
1	5,5	2	9	9	0,17	21	10	5
2	6	1,7	14	6	0,19			
3	5	2,2	10	7	0,2			
4	5,5	2	13	5	0,16			
5	5	2,8	11	6	0,24			
6	6	2	10	5	0,2			
7	5,1	1,8	16	5	0,2			
8	5	1,7	7	5	0,15			
9	5,9	2,8	10	6	0,16			
10	6	2,3	9	4	0,33			
11	6	1,9	14	7	0,17			
12	5,3	2,5	14	7	0,15			
13	5,5	2,8	11	8	0,21			
14	5,8	2,5	9	4	0,15			
15	5	2,5	11	7	0,19			
16	5	2,2	10	5	0,13			
17	5,4	2,8	10	6	0,12			
18	5,2	2,4	13	7	0,14			
19	5,8	2,6	9	10	0,2			
20	5,8	2,9	11	6	0,12			
Average	5,49	2,32	11,05	6,25	0,179			

The weights of the gabions are given in the table below.

Weights						
Weight (kg)	Empty	Oysters	Mussels	Willow wood (loose)	Willow wo	Bricks
10 cm gabion	4	20	15,7	14	14,5	64
20 cm gabion	4,5	38,5	25	26	26	127
30 cm gabion	7	55	36,5	35	36	190
40 cm gabion	8	73,5	49	45	45,5	256

8.2 Data

For all the data, the reader is referred to code,results&data and readme.txt

8.3 Code

The python codes are given below (descriptions are included in the code). For a more extensive description see code,results&data and readme.txt

8.3.1 Experiment 1

```
###--- DESCRIPTION ---###
# Calculates the mean velocity of the calibration txt - file of the vectrino with a filter
# This will be used to convert RPM to velocity

###--- IMPORT LIBRARY/MODULES ---###

import os

import pandas as pd

###--- INPUT ---###
# directory = ...:/Code,data&results/Experiment1/Data/Calibration
# Input = xxx.txt, where xxx = number of RPM

directory = 'C:\Code,data&results\Experiment1\Data\Calibration' # C-disk as an example

file = '700.txt' # 700 as an example

###--- EDIT/FILTER DATA ---###

os.chdir(directory)

df = pd.read_csv(file, sep=',', names=["CarrierPos","XPos","YPos","ZPos","Nr",
                                       "Time","Status","VelX","VelY","VelZ1",
                                       "VelZ2","Amp1","Amp2","Amp3","Amp4","SNR1",
                                       "SNR2","SNR3","SNR4","Corr1","Corr2","Corr3",
                                       "Corr4","Ch0","Ch1","Ch2","Ch3","Ch4","Ch5",
                                       "Ch6","Ch7"], dtype='a', skiprows=39)

Columns = ['VelX', 'Corr1']

for column in Columns:
    df[column] = pd.to_numeric(df[column], downcast="float") # convert from string to float

df.drop(df[df['Corr1'] <= 80].index, inplace = True) # filter out all values with a beam correlation <= 8(

###--- OUTPUT ---###
# mean of the velocity in the x-direction

print('Mean velocity of this file is ' + str(df['VelX'].mean()) + ' m/s')
```

```
###--- DESCRIPTION ---###
# Calculates the mean of a pressure measurement for the permeability measurements

###--- IMPORT LIBRARY/MODULES ---###
import numpy as np
import os

###--- INPUT ---###
# directory = ...:/Code,data&results/Experiment1/Data/Pressure
# input =  permxxxyyy.raw, where xxx = material and yyy = number or RPM

directory = 'C:\Code,data&results\Experiment1/Data/Pressure' # C-disk as an example
filename = 'permbrushloose150.raw' # example of brushloose on 150 RPM

###--- EDIT/FILTER DATA ---###

os.chdir(directory)
chan0_values_converted = []
chan1_values_converted = []
data = open(filename, 'r')

for x in data:
    list = x.split('\t')
    chan0, chan1, chan2 = list
    chan0 = float(chan0.replace(',','.'))
    chan1 = float(chan1.replace(',','.'))
    chan0_values_converted.append(chan0)
    chan1_values_converted.append(chan1)

mean = np.average(chan0_values_converted) # calculate mean
mean1 = np.average(chan1_values_converted)

###--- OUTPUT ---###
# Pressure of the sensor before the structure and pressure of the sensor after the structure

print('The pressure of the first sensor is ' + str(mean) +
      ' and the pressure of the second sensor is ' + str(mean1))
```

8.3.2 Experiment 2

```
###--- DESCRIPTION ---###
# convert all csv files of the raw data to units cm
# using the conversion factor and the mean of the data

###--- IMPORT LIBRARIES/MODULES ---###
import os
import pandas as pd
import numpy as np

###--- INPUT ---###
# complete folder with all raw data files of ...:/Code,data&results/Experiment2
# /Data/WL22cm/Raw
# and/or ...:/Code,data&results/Experiment2/Data/WL30cm/Raw
directory = r'C:\Code,data&results/Experiment2/Data/WL22cm/Raw'

###--- EDIT/FILTER DATA ---###
os.chdir(directory)
files = os.listdir('.')
con_factor_ch0 = 382.997517
con_factor_ch1 = 379.29060089999996
con_factor_ch2 = 382.68817909999996

for file in files:
    chan0_values_converted = []
    chan1_values_converted = []
    chan2_values_converted = []

    data = open(file, 'r')

    for x in data:
        list = x.split('\t')
        chan0, chan1, chan2 = list
        chan0 = float(chan0.replace(',','.')) * con_factor_ch0
        chan1 = float(chan1.replace(',','.')) * con_factor_ch1
        chan2 = float(chan2.replace(',','.')) * con_factor_ch2
        chan0_values_converted.append(chan0)
        chan1_values_converted.append(chan1)
        chan2_values_converted.append(chan2)

    mean = np.average(chan0_values_converted)
    mean1 = np.average(chan1_values_converted)
    mean2 = np.average(chan2_values_converted)

    chan0_values_converted = chan0_values_converted - mean
    chan1_values_converted = chan1_values_converted - mean1
    chan2_values_converted = chan2_values_converted - mean2

###--- OUTPUT ---###
# csv files with wave height in cm
    all_data = pd.DataFrame(data = {'chan0' : chan0_values_converted, 'chan1':
                                    chan1_values_converted,
                                'chan2' : chan2_values_converted})
    all_data.to_csv(str(file[:-4]) + '.txt', header = False, index = False,
                    sep = ',')
```

```
"""
###--- Description ---###
# Calculates the spectral significant wave height from a power spectrum created
# via a FFT for a whole folder

###--- IMPORT LIBRARIES/MODULES ---###

import os

import xlsxwriter

from scipy import signal as sp

import numpy as np

###--- INPUT ---###
# Directory: ...:/Code,data&results/Experiment2/Data/WL22cm/Converted or
# ...:/Code,data&results/Experiment2/Data/WL30cm/Converted or

directory = 'C:\Code,data&results\Experiment2\Data\WL22cm\Converted' # C-disk a

###--- EDIT/FILTER DATA ---###

os.chdir(directory )

files = os.listdir('.')

# Create excel file
workbook = xlsxwriter.Workbook('Attenuation&reflectionWL22cm.xlsx')
worksheet = workbook.add_worksheet('sig_wave_height')
worksheet.write(0,0,'filename')
worksheet.write(0,1, 'ch0')
worksheet.write(0,2, 'ch1')
worksheet.write(0,3, 'ch2')

# Read out all the converted files
for file in files:
    print(file)
    chan0_cm = []
    chan1_cm = []
    chan2_cm = []

    data = open(file, 'r')
    for x in data:
        list = x.split(',')
        chan0, chan1, chan2 = list
        chan0 = float(chan0)
        chan1 = float(chan1)
        chan2 = float(chan2)
        chan0_cm.append(chan0)
        chan1_cm.append(chan1)
        chan2_cm.append(chan2)


    delta_f = 100/1024 # = frequency/FFT length


# Calculate sectral signifanct wave height
# channel 0
    f0, amp0 = sp.welch(chan0_cm, fs = 100, nperseg = 1024)
    wave_height_direct0 = 4 * np.sqrt(np.sum(amp0) * delta_f)

# channel 1
    f1, amp1 = sp.welch(chan1_cm, fs = 100, nperseg = 1024)
    wave_height_direct1 = 4 * np.sqrt(np.sum(amp1) * delta_f)

# channel 2
    f2, amp2 = sp.welch(chan2_cm, fs = 100, nperseg = 1024)
    wave_height_direct2 = 4 * np.sqrt(np.sum(amp2) * delta_f)

# Output of an excel file with all sig_wave_heights

    worksheet.write(files.index(file) + 1, 0, file)
    worksheet.write(files.index(file) + 1, 1, wave_height_direct0)
    worksheet.write(files.index(file) + 1, 2, wave_height_direct1)
    worksheet.write(files.index(file) + 1, 3, wave_height_direct2)


workbook.close()
```

```
###--- Description ---###
# Determines the peak frequency of a signal measurement, which will be used to
# calculate wave period

###--- IMPORT LIBRARIES/MODULES

import os
from scipy import signal as sp

## INPUT ##
# Directory: ...:/Code,data&results/Experiment2/Data/WL22cm/Converted or
# ...:/Code,data&results/Experiment2/Data/WL30cm/Converted

directory = 'C:/Code,data&results/Experiment2/Data/WL22cm/Converted' # C-disk as an example
file = 'new500control.txt' # Example of the control run on 500 RPM

###--- EDIT/FILTER DATA ---###
os.chdir(directory)

chan0_cm = []
chan1_cm = []
chan2_cm = []

data = open(file, 'r')

for x in data:
    list = x.split(',')
    chan0, chan1, chan2 = list
    chan0 = float(chan0)
    chan1 = float(chan1)
    chan2 = float(chan2)
    chan0_cm.append(chan0)
    chan1_cm.append(chan1)
    chan2_cm.append(chan2)

delta_f = 100/4096 # step size of the FFT

f, amp = sp.welch(chan0_cm, fs = 100, nperseg = 4096) # generation of power spectrum

max_item = max(amp)

max_index = [index for index, item in enumerate(amp) if item == max_item] # maximum item in list

###--- OUTPUT ---###
print('The peak frequency of this file is ' + str(f[max_index]) + ' Hz')
```

8.3.3 Experiment 3

```
###--- Description ---###
# Calculates the Bed shear stress at four different positions before the structe
# of a certain material

###--- IMPORT MODULES/LIBRARIES
import numpy as np
import os
import xlsxwriter
import pandas as pd
from scipy import signal

###--- INPUT ---###
# Directory: ...:/Code,data&results/Experiment3/Data
# File: single file from the directory folder
directory = 'C:\Code,data&results\Experiment3\Data' #C-disk as an example
file = 'mussels30.txt' # mussels 30cm as an example
###--- EDIT/FILTER DATA ---###

os.chdir(directory)

 # Create excel file
Workbook = xlsxwriter.Workbook('TKE.xlsx')
worksheet = Workbook.add_worksheet('TKE')
worksheet.write(0,0,'filename')
worksheet.write(0,1, 'TKE1')
worksheet.write(0,2, 'TKE2')
worksheet.write(0,3, 'TKE3')
worksheet.write(0,3, 'TKE4')

data = pd.read_csv(file,skiprows=37)
fdata = pd.read_csv(file,skiprows=4,nrows=1,header=None)
freq = np.sum(fdata[1])
timeaxis = np.arange(0,(len(data.VelX))/freq,1/freq)

 # split the file

data1 = data.loc[:39000] # 5 cm before structure
data3 = data.loc[80000:119999] # 25 cm before structure
data5 = data.loc[160000:199999] # 45 cm before structure
data7 = data.loc[240000:279999] # 65 cm before structure
points = [data1, data3, data5, data7]

BSS = []
rho = 1025
```

```
# Apply low and high pass filter for the velocity in three different directions
# and calculate from this the bed shear stress
for point in points:
    sos1 = signal.butter(5,4,'hp',fs=200,output='sos')
    sos2 = signal.butter(5,12,'lp', fs =200, output = 'sos')
    VelX_filtered0 = signal.sosfilt(sos1,point.VelX)
    VelX_filtered = signal.sosfilt(sos2,VelX_filtered0)
    VelY_filtered0 = signal.sosfilt(sos1,point.VelY)
    VelY_filtered = signal.sosfilt(sos2,VelY_filtered0)
    VelZ_filtered0 = signal.sosfilt(sos1,point.VelZ1)
    VelZ_filtered = signal.sosfilt(sos2,VelZ_filtered0)
    varX = np.var(VelX_filtered)
    varY = np.var(VelY_filtered)
    varZ1 = np.var(VelZ_filtered)
    BSS1 = 0.5*(varX+varY+varZ1)*0.19*rho
    BSS.append(BSS1)

###--- OUTPUT ---###
 # BSS at 5, 25, 45 and 65 cm before the structure
print(BSS)
```

8.4 Results

For a more extensive description of the results, the reader is referred to code,data&results and readme.txt

8.4.1 Experiment 1

The calibration line is given in the table below. RPM manual = manual adjusted number of RPM, RPM actual = number of RPM read from the display and Velocity (m/s) = measured velocity with the vectrino.

Calibration line

RPM manual	RPM actual	Velocity (m/s) (s
100	132	0,08009629
200	254	0,184515372
300	375	0,296941847
400	477	0,405415058
500	578	0,509233773
600	676	0,603715241
700	871	0,720040262

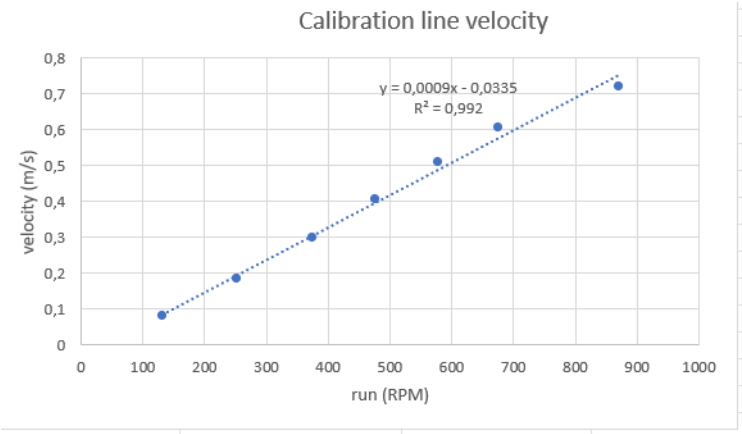

The results of experiment 1 are given below.

Run manual (RPM)	Run actual (RPM)	Velocity (m/s)	Pressure ch0 (V) (see	Pressure ch1 (V) (see	Water level ch0 (cm)	Water level ch1 (cm)	Difference water leve	Pressure difference (Pa	Permeability (m2)
0	0	0	3,8262408	3,8279007	22	22	0	0	0
150	186	0,133	3,8272267	3,825921	22,37759725	21,2491184	1,128478855	113,47137	9,7724E-07
300	375	0,3031	3,8334876	3,8206713	24,77550641	19,25795653	5,517549876	554,8034339	4,55494E-07
450	523	0,4363	3,8427502	3,8180738	28,32305921	18,27274919	10,05031001	1010,583798	3,59955E-07
0	0	0	3,7966874	3,7939661	22	22	0	0	0
150	182	0,1294	3,797465	3,7909745	22,29781887	20,86531424	1,432504631	144,0419219	7,48999E-07
300	373	0,3013	3,8026733	3,7803268	24,29258484	16,82674171	7,46584313	750,7091913	3,34629E-07
450	522	0,4354	3,8109194	3,7646986	27,45082066	10,89911234	16,55170832	1664,315651	2,18117E-07
0	0	0	3,8213846	3,8081816	22	22	0	0	0
150	184	0,1312	3,8240152	3,8056255	23,00751327	21,0304953	1,977017973	198,7940997	5,50258E-07
300	373	0,3013	3,8345557	3,7917086	27,0444986	15,75194593	11,29255266	1135,494402	2,21233E-07
450	522	0,4354	3,8454123	3,7827934	31,20254944	12,37049437	18,83205507	1893,610218	1,91705E-07
0	0	0	3,8340005	3,8322413	22	22	0	0	0
150	184	0,1312	3,8352156	3,8291784	22,46538028	20,83827082	1,627109464	163,6099244	6,6859E-07
300	373	0,3013	3,8427016	3,8192082	25,3324997	17,05666767	8,275832026	832,1555998	3,01877E-07
450	522	0,4354	3,8526725	3,811468	29,15132964	14,12088256	15,03044708	1511,34903	2,40193E-07
0	0	0	3,7974001	3,8033171	22	22	0	0	0
150	181	0,1285	3,7980816	3,8004476	22,26101281	20,91162562	1,349387187	135,6842551	7,89604E-07
300	372	0,3004	3,8033804	3,7913039	24,29044005	17,44350615	6,846933898	688,4763207	3,63787E-07
450	521	0,4345	3,8109433	3,7776476	27,18701197	12,26379992	14,92321205	1500,56628	2,41418E-07

8.4.2 Experiment 2

The results of experiment are given in the table below.

Filename	Material	Height struct	Submergence ratio (-	Peak frequency (Hz)	Wave period (s)	Hm0_ch0 (cm)	Hm0_ch1 (cm)	Hm0_ch2 (cm)	Attenuation_0	Attenuation_1	Attenuation_2	Water level	H0	ds	SR
new1000brush10.txt	brush loose	10	2,2	0,390625	2,56	9,294954344	7,153174113	5,719337238	5,595858064	-18,77192228	-33,22492386	22	8,8	12	1,36364
new1000brush20.txt	brush loose	20	1,1	0,390625	2,56	10,13742607	4,455375003	3,111513949	15,16680612	-49,40685893	-63,67208783	22	8,8	2	0,22727
new1000brush30.txt	brush loose	30	0,733333333	0,390625	2,56	11,0154044	3,725198849	2,363003908	25,14112891	-57,69839559	-72,41117994	22	8,8	-8	-0,90909
new1000brushbundled1	brush bundled	10	2,2	0,390625	2,56	9,957772238	8,99987187	6,802659389	13,12583849	2,198308072	-20,57679417	22	8,8	12	1,36364
new1000brushbundled2	brush bundled	20	1,1	0,390625	2,56	10,64704315	4,830632756	3,021131724	20,95633997	-45,14560855	-64,72732897	22	8,8	2	0,22727
new1000brushbundled3	brush bundled	30	0,733333333	0,390625	2,56	11,50600285	4,303565432	2,200712095	30,71460052	-51,13073695	-74,30598833	22	8,8	-8	-0,90909
new1000control.txt	control			0,390625	2,56	8,802385353	8,806282648	8,565077823	0	0	0	22	8,8	22	2,5
new1000hard10.txt	hard	10	2,2	0,390625	2,56	9,585303105	9,327644697	6,720383715	8,894381695	5,920341986	-21,53738875	22	8,8	12	1,36364
new1000hard20.txt	hard	20	1,1	0,390625	2,56	12,89926637	4,573207896	2,948795109	46,54285009	-48,06880407	-65,57188189	22	8,8	2	0,22727
new1000hard30.txt	hard	30	0,733333333	0,390625	2,56	15,11850486	3,960084556	1,805479106	71,75463528	-55,03114408	-78,92045883	22	8,8	-8	-0,90909
new1000mussels10.txt	mussels	10	2,2	0,390625	2,56	9,168526494	8,14447953	6,063293351	4,159567274	-7,515124643	-29,20912715	22	8,8	12	1,36364
new1000mussels20.txt	mussels	20	1,1	0,390625	2,56	9,063344797	4,505683884	2,919941325	2,964644616	-48,83557496	-65,90875897	22	8,8	2	0,22727
new1000mussels30.txt	mussels	30	0,733333333	0,390625	2,56	11,68050944	2,427597423	1,50613223	32,69709252	-72,43334651	-82,41542855	22	8,8	-8	-0,90909
new1000oysters10.txt	oysters	10	2,2	0,390625	2,56	8,888769946	8,08823151	6,241404145	0,981377085	-8,153850686	-27,12962714	22	8,8	12	1,36364
new1000oysters20.txt	oysters	20	1,1	0,390625	2,56	10,33692357	5,251065093	3,373237727	17,43320877	-40,37137686	-60,61637971	22	8,8	2	0,22727
new1000oysters30.txt	oysters	30	0,733333333	0,390625	2,56	12,09571738	4,52382478	2,327562201	37,41408602	-48,62957548	-72,82497311	22	8,8	-8	-0,90909
new1250brush10.txt	brush loose	10	2,2	0,48828125	2,048	7,32787414	5,816474949	4,084117959	12,98493562	-15,59069271	-29,50154679	22	6,49	12	1,849
new1250brush20.txt	brush loose	20	1,1	0,48828125	2,048	7,403276513	3,52870119	2,135320821	14,14752822	-48,79111048	-63,14092381	22	6,49	2	0,30817
new1250brush30.txt	brush loose	30	0,733333333	0,48828125	2,048	7,981091537	2,877499769	1,587949134	23,0565777	-58,24141522	-72,58944064	22	6,49	-8	-1,23267
new1250brushbundled1	brush bundled	10	2,2	0,48828125	2,048	7,946399001	6,236048242	4,608204771	22,52167032	-9,501800141	-20,45496439	22	6,49	12	1,849
new1250brushbundled2	brush bundled	20	1,1	0,48828125	2,048	8,012491462	3,902676997	2,151451963	23,5407179	-43,36393351	-62,86247433	22	6,49	2	0,30817
new1250brushbundled3	brush bundled	30	0,733333333	0,48828125	2,048	8,663701191	3,188985645	1,457932913	33,58140473	-53,72109884	-74,83373001	22	6,49	-8	-1,23267
new1250control.txt	control			0,48828125	2,048	6,485709002	6,890798106	5,793202223	0	0	0	22	6,49	22	3,38983
new1250hard10.txt	hard	10	2,2	0,48828125	2,048	7,753165375	6,72263697	4,524133041	19,5422948	-2,440372414	-21,90617785	22	6,49	12	1,849
new1250hard20.txt	hard	20	1,1	0,48828125	2,048	9,192524277	3,608420755	2,460992192	41,73507128	-47,63421161	-57,51931149	22	6,49	2	0,30817
new1250hard30.txt	hard	30	0,733333333	0,48828125	2,048	12,34670361	2,942393455	1,164176648	90,36783184	-57,2996711	-79,90443621	22	6,49	-8	-1,23267
new1250mussels10.txt	mussels	10	2,2	0,48828125	2,048	7,115227648	6,050725111	4,045111757	9,706242538	-12,19122927	-30,17485666	22	6,49	12	1,849
new1250mussels20.txt	mussels	20	1,1	0,48828125	2,048	6,554386715	3,539099163	2,031372673	1,058908338	-48,64021397	-64,93523625	22	6,49	2	0,30817
new1250mussels30.txt	mussels	30	0,733333333	0,48828125	2,048	8,175013289	1,812124673	0,964922221	26,04656309	-73,7022527	-83,34388852	22	6,49	-8	-1,23267
new1250oysters10.txt	oysters	10	2,2	0,48828125	2,048	7,150113412	5,985454937	4,355308044	10,24412921	-13,13843702	-24,82036919	22	6,49	12	1,849
new1250oysters20.txt	oysters	20	1,1	0,48828125	2,048	7,759042887	4,109679583	2,361201694	19,63291731	-40,35988982	-59,24185619	22	6,49	2	0,30817
new1250oysters30.txt	oysters	30	0,733333333	0,48828125	2,048	9,347398149	3,42296389	1,541857043	44,12299636	-50,32558149	-73,38506436	22	6,49	-8	-1,23267
new500brush10.txt	brush loose	10	2,2	0,1953125	5,12	5,294062277	5,095175948	4,298963115	3,87072176	-0,181897724	-14,42264919	22	5,1	12	2,35294
new500brush20.txt	brush loose	20	1,1	0,1953125	5,12	5,795369401	4,272402514	2,443521471	13,70648305	-16,30061152	-51,35801622	22	5,1	2	0,39216
new500brush30.txt	brush loose	30	0,733333333	0,1953125	5,12	7,538902418	4,655574514	2,041630556	47,91500261	-8,794000886	-59,35826159	22	5,1	-8	-1,56863
new500brushbundled1(	brush bundled	10	2,2	0,1953125	5,12	6,790308527	6,055800696	4,544529552	33,22741797	18,63742084	-9,534278536	22	5,1	12	2,35294
new500brushbundled2(	brush bundled	20	1,1	0,1953125	5,12	5,942760168	4,502961874	2,259408744	16,59832387	-11,78379051	-55,02305799	22	5,1	2	0,39216
new500brushbundled3(	brush bundled	30	0,733333333	0,1953125	5,12	6,85076762	4,740840417	2,098640609	34,4136393	-7,123581514	-58,22339043	22	5,1	-8	-1,56863
new500control.txt	control			0,1953125	5,12	5,0967801	5,104460846	5,023482352	0	0	0	22	5,1	22	4,31373
new500hard10.txt	hard	10	2,2	0,1953125	5,12	6,833066485	5,80926731	4,34072854	34,06633896	13,80765736	-13,59124535	22	5,1	12	2,35294
new500hard20.txt	hard	20	1,1	0,1953125	5,12	8,437956905	5,998596878	2,172818267	65,55465882	17,51675756	-56,74677216	22	5,1	2	0,39216
new500hard30.txt	hard	30	0,733333333	0,1953125	5,12	14,25740021	7,176974879	1,52003978	179,7334774	40,60201646	-69,74131343	22	5,1	-8	-1,56863
new500mussels10.txt	mussels	10	2,2	0,1953125	5,12	6,257082887	5,897108442	4,251907361	22,76540803	15,52852729	-15,35936502	22	5,1	12	2,35294
new500mussels20.txt	mussels	20	1,1	0,1953125	5,12	6,098553378	4,863410852	2,106895521	19,65502255	-4,72233996	-58,05906394	22	5,1	2	0,39216
new500mussels30.txt	mussels	30	0,733333333	0,1953125	5,12	7,206741697	3,922256558	1,496189567	41,39793273	-23,16021856	-70,21608792	22	5,1	-8	-1,56863
new500oysters10.txt	oysters	10	2,2	0,1953125	5,12	5,82817197	5,28919259	4,151303014	14,35007702	3,619025581	-17,36204643	22	5,1	12	2,35294
new500oysters20.txt	oysters	20	1,1	0,1953125	5,12	5,943922584	4,629905452	2,464991556	16,62113075	-9,296875983	-50,93062176	22	5,1	2	0,39216
new500oysters30.txt	oysters	30	0,733333333	0,1953125	5,12	6,997745439	5,020631564	2,095729548	37,29737799	-1,642274966	-58,28133949	22	5,1	-8	-1,56863
new750brush10.txt	brush loose	10	2,2	0,29296875	3,413333333	8,415181234	6,003272135	5,310387456	-16,68839797	-17,33358775	-34,16474044	22	10,1	12	1,18812
new750brush20.txt	brush loose	20	1,1	0,29296875	3,413333333	8,202778087	4,394526601	2,992990236	-18,79122214	-39,48637686	-62,89455512	22	10,1	2	0,19802
new750brush30.txt	brush loose	30	0,733333333	0,29296875	3,413333333	9,725632326	4,019025389	2,274269647	-3,714728505	-44,65711329	-71,80485722	22	10,1	-8	-0,79208
new750brushbundled1(	brush bundled	10	2,2	0,29296875	3,413333333	10,27127975	7,151633134	6,296364321	1,687265757	-1,520397612	-21,9411422	22	10,1	12	1,18812
new750brushbundled2(	brush bundled	20	1,1	0,29296875	3,413333333	8,517830212	4,550918958	2,83237256	-15,67215714	-37,3328188	-64,88580463	22	10,1	2	0,19802
new750brushbundled3(	brush bundled	30	0,733333333	0,29296875	3,413333333	9,570130217	4,445826091	2,243647212	-5,254223559	-38,77997129	-72,18449731	22	10,1	-8	-0,79208
new750control.txt	control			0,29296875	3,413333333	10,10085154	7,262045094	8,066175317	0	0	0	22	10,1	22	2,17822
new750hard10.txt	hard	10	2,2	0,29296875	3,413333333	9,399694219	6,929292691	5,904461935	-6,941566422	-4,58207569	-26,79973218	22	10,1	12	1,18812
new750hard20.txt	hard	20	1,1	0,29296875	3,413333333	11,00963247	5,388593204	3,226544261	8,997072486	-25,79785537	-59,99908093	22	10,1	2	0,19802
new750hard30.txt	hard	30	0,733333333	0,29296875	3,413333333	18,08497577	6,817256975	1,931525711	79,04407071	-6,124832792	-76,05400782	22	10,1	-8	-0,79208
new750mussels10.txt	mussels	10	2,2	0,29296875	3,413333333	8,595059563	6,560018149	5,235622323	-14,90757456	-9,667069477	-35,09163739	22	10,1	12	1,18812
new750mussels20.txt	mussels	20	1,1	0,29296875	3,413333333	7,36143506	4,236779115	2,57266086	-27,12064886	-41,65859534	-68,10556727	22	10,1	2	0,19802
new750mussels30.txt	mussels	30	0,733333333	0,29296875	3,413333333	9,795413567	2,861515946	1,560760785	-3,02388338	-60,59627957	-80,65054721	22	10,1	-8	-0,79208
new750oysters10.txt	oysters	10	2,2	0,29296875	3,413333333	8,415305171	6,145686921	5,603837063	-16,68717098	-15,37250401	-30,5267138	22	10,1	12	1,18812
new750oysters20.txt	oysters	20	1,1	0,29296875	3,413333333	8,507428271	4,878307329	3,145114839	-15,77513797	-32,82460704	-61,00859805	22	10,1	2	0,19802
new750oysters30.txt	oysters	30	0,733333333	0,29296875	3,413333333	9,591070168	4,605418461	2,310753111	-5,046914786	-36,58234834	-71,35255533	22	10,1	-8	-0,79208
1000brush10.txt	brush loose	10	3	0,390625	2,56	9,527449462	11,45249036	5,55620157	-10,67609929	-4,270907534	-19,03169239	30	10,67	20	1,87441
1000brush20.txt	brush loose	20	1,5	0,390625	2,56	10,55381165	10,55422868	4,438886518	-1,053516208	-11,77929849	-35,31387864	30	10,67	10	0,93721
1000brush30.txt	brush loose	30	1	0,390625	2,56	11,49858003	8,303810795	2,523486944	7,804090198	-30,59009467	-63,22623207	30	10,67	0	0
1000brush40.txt	brush loose	40	0,75	0,390625	2,56	12,98013989	8,392698565	1,807168001	21,69434553	-29,84709946	-73,66486209	30	10,67	-10	-0,93721
1000brushbundled10.t	brush bundled	10	3	0,390625	2,56	9,496487003	11,36720239	5,695913831	-10,96638554	-4,983812725	-16,99572138	30	10,67	20	1,87441
1000brushbundled20.t	brush bundled	20	1,5	0,390625	2,56	9,174510626	10,34776552	4,315761131	-13,98505136	-13,50508304	-37,10813576	30	10,67	10	0,93721
1000brushbundled30.t	brush bundled	30	1	0,390625	2,56	11,4859747	8,607946329	2,432190991	7,685909783	-28,04788615	-64,55665155	30	10,67	0	0
1000brushbundled40.t	brush bundled	40	0,75	0,390625	2,56	13,87839489	7,083600006	2,86105774	30,11586906	-40,78959433	-58,3069476	30	10,67	-10	-0,93721
1000control.txt	control			0,390625	2,56	10,6661816	11,96343772	6,862193041	0	0	0	30	10,67	30	2,81162
1000hard10.txt	hard	10	3	0,390625	2,56	9,307019141	12,30862242	6,036528958	-12,74272754	2,885330369	-12,0320731	30	10,67	20	1,87441
1000hard20.txt	hard	20	1,5	0,390625	2,56	10,99688863	10,40740751	3,582785964	3,100519426	-13,00654749	-47,78949028	30	10,67	10	0,93721
1000hard30.txt	hard	30	1	0,390625	2,56	15,18882812	6,95710639	2,574320086	42,40173937	-41,84692935	-62,48546097	30	10,67	0	0
1000hard40.txt	hard	40	0,75	0,390625	2,56	16,85861954	6,499352676	2,513939453	58,05674585	-45,67320173	-63,36536384	30	10,67	-10	-0,93721
1000mussels10.txt	mussels	10	3	0,390625	2,56	8,799187256	11,55698576	5,866561328	-17,50386796	-3,397451224	-14,50894352	30	10,67	20	1,87441

1000mussels20.txt	mussels	20	1,5	0,390625	2,56	9,669816919	9,513010878	3,522024079	-9,341343689	-20,48263132	-48,67494898	30	10,67	10	0,93721
1000mussels30.txt	mussels	30	1	0,390625	2,56	10,39817842	4,565232737	1,984979341	-2,512644079	-61,84012619	-71,0736884	30	10,67	0	0
1000mussels40.txt	mussels	40	0,75	0,390625	2,56	14,64529352	4,002260635	2,58244396	37,3058707	-66,54589819	-62,367075	30	10,67	-10	-0,93721
1000oysters10.txt	oysters	10	3	0,390625	2,56	9,255340717	11,65948682	6,027798667	-13,22723479	-2,540665204	-12,15929614	30	10,67	20	1,87441
1000oysters20.txt	oysters	20	1,5	0,390625	2,56	10,87413771	9,863863751	4,582395777	1,9496772	-17,54992184	-33,2225755	30	10,67	10	0,93721
1000oysters30.txt	oysters	30	1	0,390625	2,56	12,63901711	7,566178372	2,836917741	18,49617404	-36,75581761	-58,65873017	30	10,67	0	0
1000oysters40.txt	oysters	40	0,75	0,390625	2,56	13,50105329	7,11214282	2,131487685	26,57813069	-40,55101061	-68,9386808	30	10,67	-10	-0,93721
1250brush10.txt	brush loose	10	3	0,48828125	2,048	7,322071547	9,780618979	4,915950488	0,48404065	4,465986979	-18,66023155	30	7,29	20	2,74348
1250brush20.txt	brush loose	20	1,5	0,48828125	2,048	8,423396709	8,24941502	3,961662436	15,59801511	-11,88867658	-34,44996934	30	7,29	10	1,37174
1250brush30.txt	brush loose	30	1	0,48828125	2,048	9,529366397	6,166583788	1,972175251	30,77572846	-34,13522569	-67,3682071	30	7,29	0	0
1250brush40.txt	brush loose	40	0,75	0,48828125	2,048	10,3916433	6,072182616	1,603547338	42,60913747	-35,14351684	-73,46755841	30	7,29	-10	-1,37174
1250brushbundled10.tx	brush bundled	10	3	0,48828125	2,048	7,149357575	9,668863146	4,857846954	-1,886189926	3,272332114	-19,62161796	30	7,29	20	2,74348
1250brushbundled20.tx	brush bundled	20	1,5	0,48828125	2,048	7,800831341	8,214235666	3,636053758	7,054273979	-12,26442437	-39,83752044	30	7,29	10	1,37174
1250brushbundled30.tx	brush bundled	30	1	0,48828125	2,048	9,345720955	6,230775433	2,146674628	28,25548047	-33,4496	-64,48092438	30	7,29	0	0
1250brushbundled40.tx	brush bundled	40	0,75	0,48828125	2,048	10,72772775	5,472504873	1,222246777	47,22137364	-41,54862549	-79,77659252	30	7,29	-10	-1,37174
1250control.txt				0,48828125	2,048	7,286800471	9,362491335	6,043723239	0	0	0	30	7,29	30	4,11523
1250hard10.txt	hard	10	3	0,48828125	2,048	7,596400756	10,51595152	4,928220024	4,248782257	12,32001334	-18,45721868	30	7,29	20	2,74348
1250hard20.txt	hard	20	1,5	0,48828125	2,048	10,37870375	6,983221176	3,213008496	42,43156221	-25,4127889	-46,83726621	30	7,29	10	1,37174
1250hard30.txt	hard	30	1	0,48828125	2,048	12,09479273	4,426996163	1,008074334	65,98221367	-52,71561805	-83,32030944	30	7,29	0	0
1250hard40.txt	hard	40	0,75	0,48828125	2,048	13,54176524	3,542234509	1,173867477	85,83966034	-62,16568452	-80,57708087	30	7,29	-10	-1,37174
1250mussels10.txt	mussels	10	3	0,48828125	2,048	6,79998918	10,04260661	4,976074985	-6,680727608	7,264255344	-17,6654061	30	7,29	20	2,74348
1250mussels20.txt	mussels	20	1,5	0,48828125	2,048	9,356244168	6,66202387	2,988005957	28,39989519	-28,84347091	-50,56017889	30	7,29	10	1,37174
1250mussels30.txt	mussels	30	1	0,48828125	2,048	8,507502646	2,431241425	1,308707555	16,75223824	-74,03211027	-78,34600456	30	7,29	0	0
1250mussels40.txt	mussels	40	0,75	0,48828125	2,048	11,09107159	2,285607925	1,103238856	52,20770256	-75,58760972	-81,74570852	30	7,29	-10	-1,37174
1250oysters20.txt	oysters	20	1,5	0,48828125	2,048	9,437758873	8,086402677	3,922174862	29,51855771	-13,62979801	-35,10333437	30	7,29	10	1,37174
1250oysters30.txt	oysters	30	1	0,48828125	2,048	10,22080833	5,411834126	2,003363431	40,26469328	-42,19664476	-66,85216461	30	7,29	0	0
1250oysters40.txt	oysters	40	0,75	0,48828125	2,048	11,10095859	4,896239146	1,359701424	52,3433863	-47,70367234	-77,5022553	30	7,29	-10	-1,37174
500brush10.txt	brush loose	10	3	0,1953125	5,12	7,412503005	5,581944959	5,656427596	22,19491261	-0,529027811	-24,22437423	30	6,07	20	3,29489
500brush20.txt	brush loose	20	1,5	0,1953125	5,12	9,381699987	6,886291909	5,550900932	54,65707188	22,71460145	-25,638049	30	6,07	10	1,64745
500brush30.txt	brush loose	30	1	0,1953125	5,12	11,07542435	6,202427741	4,240032381	82,57807242	10,52805461	-43,1989358	30	6,07	0	0
500brush40.txt	brush loose	40	0,75	0,1953125	5,12	11,65369265	5,847506582	3,568444061	92,11080976	4,203314234	-52,19578485	30	6,07	-10	-1,64745
500brushbundled10.txt	brush bundled	10	3	0,1953125	5,12	7,145476675	5,463481384	6,023258644	17,79299075	-2,640063848	-19,3101679	30	6,07	20	3,29489
500brushbundled20.txt	brush bundled	20	1,5	0,1953125	5,12	8,089934796	5,82252954	5,211690055	33,36235745	3,758220143	-30,18224514	30	6,07	10	1,64745
500brushbundled30.txt	brush bundled	30	1	0,1953125	5,12	10,20997198	6,682829224	4,171120609	68,31111335	19,0888704	-44,12210376	30	6,07	0	0
500brushbundled40.txt	brush bundled	40	0,75	0,1953125	5,12	14,22322039	6,368406126	4,117349765	134,4694055	13,48581064	-44,84243815	30	6,07	-10	-1,64745
500control.txt				0,1953125	5,12	6,066130616	5,611632054	7,464705884	0	0	0	30	6,07	30	4,94234
500hard10.txt	hard	10	3	0,1953125	5,12	8,225721441	6,045606213	5,874769871	35,60079665	7,733474957	-21,29937921	30	6,07	20	3,29489
500hard20.txt	hard	20	1,5	0,1953125	5,12	10,30697546	6,419510241	4,710124014	69,91021323	14,39649249	-36,90141197	30	6,07	10	1,64745
500hard30.txt	hard	30	1	0,1953125	5,12	13,93586283	7,074638825	2,856337411	129,7323238	26,07096754	-61,73543264	30	6,07	0	0
500hard40.txt	hard	40	0,75	0,1953125	5,12	15,52014722	6,293827581	1,909414054	155,8492093	12,15681144	-74,42077312	30	6,07	-10	-1,64745
500mussels10.txt	mussels	10	3	0,1953125	5,12	7,518802834	6,255927172	6,257164831	23,94726244	11,48142131	-16,17667289	30	6,07	20	3,29489
500mussels20.txt	mussels	20	1,5	0,1953125	5,12	10,39868031	7,053157355	5,107361615	71,42196506	25,688165	-31,57986806	30	6,07	10	1,64745
500mussels30.txt	mussels	30	1	0,1953125	5,12	11,45590242	5,210842734	2,389096604	88,85024318	-7,142116863	-67,99476575	30	6,07	0	0
500mussels40.txt	mussels	40	0,75	0,1953125	5,12	14,93530456	4,189224713	2,326976443	146,2080939	-25,3474805	-68,82695073	30	6,07	-10	-1,64745
500oysters10.txt	oysters	10	3	0,1953125	5,12	7,468598025	6,346723118	6,428449003	23,11963751	13,09941666	-13,88208587	30	6,07	20	3,29489
500oysters20.txt	oysters	20	1,5	0,1953125	5,12	8,525128617	8,750805256	5,543786944	40,53651589	55,94046744	-25,73335064	30	6,07	10	1,64745
500oysters30.txt	oysters	30	1	0,1953125	5,12	12,38677571	6,437849863	4,547439643	104,1956644	14,7233069	-39,08079281	30	6,07	0	0
500oysters40.txt	oysters	40	0,75	0,1953125	5,12	13,86755967	5,698129746	3,633953208	128,6063481	1,541399938	-51,31819975	30	6,07	-10	-1,64745
750brush10.txt	brush loose	10	3	0,29296875	3,413333333	15,61182538	12,00658682	8,424520921	2,305942782	18,35632782	-28,48398456	30	15,26	20	1,31062
750brush20.txt	brush loose	20	1,5	0,29296875	3,413333333	15,96715501	11,84994611	6,662498967	4,634455408	16,81222374	-43,44184275	30	15,26	10	0,65531
750brush30.txt	brush loose	30	1	0,29296875	3,413333333	15,60249235	10,03388858	3,651182761	2,244782456	-1,08977484	-69,00499802	30	15,26	0	0
750brush40.txt	brush loose	40	0,75	0,29296875	3,413333333	17,37446518	9,334369871	2,497681296	13,85670784	-7,985361966	-78,79710718	30	15,26	-10	-0,65531
750brushbundled10.txt	brush bundled	10	3	0,29296875	3,413333333	15,57561215	11,59055164	8,640888838	2,06863366	14,25521259	-26,64723071	30	15,26	20	1,31062
750brushbundled20.txt	brush bundled	20	1,5	0,29296875	3,413333333	14,69826014	11,78224926	6,898385352	-3,68074684	16,14489423	-41,43939603	30	15,26	10	0,65531
750brushbundled30.txt	brush bundled	30	1	0,29296875	3,413333333	15,60258631	10,89017658	3,912665241	2,245398213	7,351183843	-66,78526525	30	15,26	0	0
750brushbundled40.txt	brush bundled	40	0,75	0,29296875	3,413333333	17,59994937	8,591795554	3,369959746	15,33432957	-15,30537477	-71,39230878	30	15,26	-10	-0,65531
750control.txt				0,29296875	3,413333333	15,2599399	10,14444013	11,77990814	0	0	0	30	15,26	30	1,96592
750hard10.txt	hard	10	3	0,29296875	3,413333333	16,04838759	12,88626244	8,738215063	5,166781116	27,02783266	-25,82102541	30	15,26	20	1,31062
750hard20.txt	hard	20	1,5	0,29296875	3,413333333	15,65863076	13,72114959	5,84258779	2,612663389	35,25782995	-50,40209378	30	15,26	10	0,65531
750hard30.txt	hard	30	1	0,29296875	3,413333333	18,837456	9,664981304	2,948111834	23,44384139	-4,726321255	-74,97338859	30	15,26	0	0
750hard40.txt	hard	40	0,75	0,29296875	3,413333333	19,85543849	8,876243245	2,981277252	30,11478829	-12,50139853	-74,69184634	30	15,26	-10	-0,65531
750mussels10.txt	mussels	10	3	0,29296875	3,413333333	15,19873606	12,13600453	8,64909883	-0,401075208	19,63207799	-26,57753584	30	15,26	20	1,31062
750mussels20.txt	mussels	20	1,5	0,29296875	3,413333333	14,66806848	12,84981755	5,832517003	-3,878595997	26,66857297	-50,487585	30	15,26	10	0,65531
750mussels30.txt	mussels	30	1	0,29296875	3,413333333	14,73555773	7,295051002	2,981557271	-3,436331803	-28,0881852	-74,68946925	30	15,26	0	0
750mussels40.txt	mussels	40	0,75	0,29296875	3,413333333	18,48235355	5,177589276	3,067426571	21,11681746	-48,96131076	-73,96052214	30	15,26	-10	-0,65531
750oysters10.txt	oysters	10	3	0,29296875	3,413333333	15,73299926	12,27582312	8,785806294	3,100008023	21,01035603	-25,417022	30	15,26	20	1,31062
750oysters20.txt	oysters	20	1,5	0,29296875	3,413333333	16,23108241	11,83356791	6,471385369	6,363999585	16,65077374	-45,06421193	30	15,26	10	0,65531
750oysters30.txt	oysters	30	1	0,29296875	3,413333333	16,62730541	9,544738768	3,513012858	8,960490834	-5,911626057	-70,17792654	30	15,26	0	0
750oysters40.txt	oysters	40	0,75	0,29296875	3,413333333	17,5843706	8,187222937	2,499057451	15,23224021	-19,29349646	-78,78542496	30	15,26	-10	-0,65531

8.4.3 Experiment 3

The results of experiment 3 are given in the table below.

filename	material	x position	BSS
control.txt	control	-5	0,021208
control.txt	control	-25	0,013121
control.txt	control	-45	0,016141
control.txt	control	-65	0,015861
hard30.txt	hard	-5	0,095835
hard30.txt	hard	-25	0,040993
hard30.txt	hard	-45	0,028424
hard30.txt	hard	-65	0,022971
brushloose30.txt	brush loose	-5	0,03965
brushloose30.txt	brush loose	-25	0,037513
brushloose30.txt	brush loose	-45	0,025445
brushloose30.txt	brush loose	-65	0,022619
brushbundled30.txt	brush bundled	-5	0,024365
brushbundled30.txt	brush bundled	-25	0,037333
brushbundled30.txt	brush bundled	-45	0,025012
brushbundled30.txt	brush bundled	-65	0,022317
oysters30.txt	oysters	-5	0,058786
oysters30.txt	oysters	-25	0,0347
oysters30.txt	oysters	-45	0,024372
oysters30.txt	oysters	-65	0,020331
mussels30.txt	mussels	-5	0,009245
mussels30.txt	mussels	-25	0,02968
mussels30.txt	mussels	-45	0,026497
mussels30.txt	mussels	-65	0,022191